

Channel Reconstruction-Based Hybrid Precoding for Millimeter Wave Multi-User MIMO Systems

Miguel R. Castellanos[†], Vasanthan Raghavan^{*}, Jung H. Ryu^{*},
Ozge H. Koymen^{*}, Junyi Li^{*}, David J. Love[†], and Borja Peleato[†]

[†]Purdue University, West Lafayette, IN 47907, USA

^{*}Qualcomm Corporate R&D, Bridgewater, NJ 08807, USA

Abstract

The focus of this paper is on multi-user multi-input multi-output (MIMO) transmissions for millimeter wave systems with a hybrid precoding architecture at the base-station. To enable multi-user transmissions, the base-station uses a cell-specific codebook of beamforming vectors over an initial *beam alignment* phase. Each user uses a user-specific codebook of beamforming vectors to learn the top- P (where $P \geq 1$) beam pairs in terms of the observed signal-to-noise ratio (SNR) in a single-user setting. The top- P beam indices along with their SNRs are fed back from each user and the base-station leverages this information to generate beam weights for simultaneous transmissions. A typical method to generate the beam weights is to use *only* the best beam for each user and either steer energy along this beam, or to utilize this information to reduce multi-user interference. The other beams are used as fall back options to address blockage or mobility. Such an approach completely discards information learned about the channel condition(s) even though each user feeds back this information. With this background, this work develops an advanced *directional* precoding structure for simultaneous transmissions at the cost of an additional marginal feedback overhead. This construction relies on three main innovations: 1) Additional feedback to allow the base-station to *reconstruct* a rank- P approximation of the channel matrix between it and each user, 2) A zeroforcing structure that leverages this information to combat multi-user interference by remaining agnostic of the receiver beam knowledge in the precoder design, and 3) A hybrid precoding architecture that allows *both* amplitude and phase control at low-complexity

and cost to allow the implementation of the zeroforcing structure. Numerical studies show that the proposed scheme results in a significant sum rate performance improvement over naïve schemes even with a coarse initial beam alignment codebook.

Index Terms

Millimeter wave, multi-input multi-output, multi-user, beamforming, hybrid precoding, phase and amplitude control, zeroforcing, generalized eigenvector, channel estimation

I. INTRODUCTION

Over the last few years, there has been a growing interest in leveraging the opening up of the spectrum in the millimeter wave band (~ 30 -100 GHz) in realizing the emerging higher data rate demands of cellular systems [1]–[4]. Communications in the millimeter wave band suffers from increased path loss exponents, higher shadow fading, blockage and penetration losses, etc., than sub-6 GHz systems leading to a poorer link margin than legacy systems [5]–[10]. However, by restricting attention to small cell coverage and by reaping the increased array gains from the use of large antenna arrays at both the base-station and user ends, significant rate improvements can be realized in practice.

Millimeter wave propagation is spatially *sparse* with few dominant clusters in the channel relative to the number of antennas [5], [6], [11], [12]. Spatial sparsity of the channel along with the use of large antenna arrays motivates a subset of physical layer beamforming schemes based on *directional* transmissions for signaling. In this context, there have been a number of studies on the design and performance analysis of directional beamforming/precoding structures for single-user multi-input multi-output (MIMO) systems [13]–[22]. These works [16]–[19] show that directional schemes are not only good from an implementation standpoint, but are also robust to phase changes across clusters and allow a smooth tradeoff between peak beamforming gain and initial user discovery latency. There has also been progress in generalizing such directional constructions for multi-user MIMO transmissions [22]–[25].

In this context, while legacy systems use as many radio frequency (RF) chains¹ as the number of antennas, their higher cost, energy consumption, area and weight at millimeter wave carrier frequencies has resulted in the popularity of *hybrid beamforming* systems [26]–[29]. A hybrid

¹An RF chain includes (but is not limited to) analog-to-digital converters (ADCs), digital-to-analog converters (DACs), mixers, low-noise and power amplifiers (PAs), etc.

beamforming system uses a smaller number of RF chains than the number of antennas, with the one extreme case of a single RF chain being called the analog/RF beamforming system and the other extreme of as many RF chains as the number of antennas being called the digital beamforming system. Spatial sparsity of millimeter wave channels ensures that having as many RF chains as the number of dominant clusters in the channel is sufficient to reap the full array gain possible over these channels.

A number of recent works have addressed hybrid beamforming for millimeter wave systems. The problem of finding the optimal precoder and combiner with a hybrid architecture is posed as a sparse reconstruction problem in [17], leading to algorithms and solutions based on basis pursuit methods. While the solutions achieve good performance in certain cases, to address the performance gap between the solution proposed in [17] and the unconstrained beamformer structure, an iterative scheme is proposed in [30], [31] relying on a hierarchical training codebook for adaptive estimation of millimeter wave channels. The authors in [30], [31] show that a few iterations of the scheme are sufficient to achieve near-optimal performance. In [32], it is established that a hybrid architecture can approach the performance of a digital architecture as long as the number of RF chains is twice that of the data-streams. A heuristic algorithm with good performance is developed when this condition is not satisfied. A number of other works such as [33]–[36] have also explored iterative/algorithmic solutions for hybrid beamforming.

A common theme that underlies most of these works is the assumption of *phase-only* control in the RF/analog domain for the hybrid beamforming architecture. This assumption makes sense at the user end with a smaller number of antennas (relative to the base-station end), where operating the PAs below their peak rating across RF chains can lead to a substantially poor uplink performance. On the other hand, amplitude control (denoted as *amplitude tapering* in the antenna theory literature) is necessary at the base-station end with a large number of antennas for side-lobe management and mitigating out-of-band emissions. Further, given that the base-station is a network resource, simultaneous amplitude and phase control of the individual antennas across RF chains is feasible at millimeter wave base-stations at a low-complexity² and cost [37, pp. 285-289], [38], [39]. In particular, the millimeter wave experimental prototype demonstrated in [40] allows simultaneous amplitude and phase control. Thus, it is important to consider a hybrid architecture with these constraints. Further, given the directional nature of the channel,

²Any calibration complexity can be seen as a one-time effort at the unit level for a large array and defrayed as a low network cost.

a solution should both inherit a directional structure and provide an intuitive description of the beam weights. For example, a *black box*-type algorithmic solution that does not provide an intuitive description of the beam weights is less preferable over a solution that is constructed out of measurement reports obtained over an initial *beam alignment* phase with a directional structure for the sounding beams.

Main Contributions: With this backdrop, this work addresses these two fundamental issues in hybrid beamformer design. It is assumed that the base-station trains all the users in the cell with a cell-specific codebook of beamforming vectors over an initial beam alignment phase. Each user makes an estimate³ of the top- P (where $P \geq 1$) beams over this phase and reports the beam indices to be used by the base-station as well as the measured/received signal-to-noise ratios (SNRs). The simplest implementation at the base-station uses only the best beam information for beam steering or zeroforcing as in [23], [24], with other beams serving as fall back options.

In contrast to this approach, we propose to *reconstruct* or *estimate* a rank- P approximation of the channel matrix between the base-station and the user (at the base-station end). To realize this reconstruction, we envision the additional feedback of the phase of the received signal estimate of the top- P beams over the beam alignment phase and the cross-correlation information of the top- P beams at the user end with the beam used for multi-user reception. With this novel construction, the base-station can remain agnostic of the user's top- P beams in precoder design. In terms of overhead, in 3GPP 5G-NR, these quantities can be fed back over the physical uplink control channel (PUCCH) with a Type-II feedback scheme [41, Sec. 8.2.1.6.3, pp. 24-26]; see Sec. V-C for a detailed study that demonstrates this feedback overhead to be marginal. Leveraging the rank- P channel approximation, we propose the use of a zeroforcing structure that is then quantized to meet the RF precoding constraints (amplitude and phase control) at the base-station end for simultaneous transmissions.

To benchmark and compare the performance of the proposed scheme, we establish two upper bounds for the sum rate. This is a fundamentally difficult problem given the non-convex dependence of the sum rate on the beamforming vectors [42]–[44]. The first bound is based on an intuitive parsing and understanding of the zeroforcing structure. The second bound is

³In a practical implementation such as the Third Generation Partnership Project New Radio (3GPP 5G-NR) design, $P = 4$ is typically assumed both in terms of measurements and reporting [41]. The received SNR is estimated as the received power of a beamformed link (corresponding to the beam pair under consideration) using a certain reference symbol resource. This metric is typically known as the reference symbol received power (RSRP) of the link.

based on an alternating optimization of the beamformer-combiner pair with signal-to-leakage and noise ratio (SLNR) [45] and signal-to-interference and noise ratio (SINR) as optimization metrics. Numerical studies show that the proposed scheme performs significantly better than a naïve beam steering solution even for an initial beam alignment codebook of poor resolution. Further, the proposed scheme is comparable with the established upper bounds provided the beam alignment codebook resolution is moderate-to-good. Thus, our work establishes the utility and efficacy of the proposed feedback techniques as well as opens up avenues for further investigation of such approaches in hybrid beamforming with millimeter wave systems.

Organization: This paper is organized as follows. Sec. II develops the system setup and explains the RF precoder architectural constraints adopted in this work. In Sec. III, we provide a background of the initial beam alignment phase and the feedback mechanism necessary for the multi-user beamforming envisioned in this work. Sec. IV generates two upper bounds on the sum rate to benchmark the performance of the proposed scheme. Sec. V performs a number of numerical studies to understand the performance of the proposed scheme relative to a naïve beam steering solution as well as to the upper bounds developed in Sec. IV. Concluding remarks are provided in Sec. VI.

Notations: Lower- and upper-case bold symbols are used to denote vectors and matrices, respectively. The i -th entry of a vector \mathbf{x} and the (i, j) -th entry of a matrix \mathbf{X} are denoted by $\mathbf{x}(i)$ and $\mathbf{X}(i, j)$, respectively. The regular matrix transpose and complex conjugate Hermitian transpose operations of a matrix are denoted by $(\cdot)^T$ and $(\cdot)^\dagger$, respectively. The two-norm of a vector is denoted as $\|\cdot\|$ with \mathbb{C} , \mathbb{R} and \mathcal{CN} standing for the set of reals, complex numbers and the complex normal random variable, respectively.

II. SYSTEM SETUP

We consider a cellular downlink scenario with a single base-station serving K_{cell} potential users. The base-station and each user are assumed to be equipped with planar arrays of dimensions $N_{\text{tx}} \times N_{\text{tz}}$ antennas and $N_{\text{rx}} \times N_{\text{rz}}$ antennas, respectively. At both ends, the inter-antenna element spacing is $\lambda/2$ where λ is the wavelength of propagation. With $N_{\text{t}} = N_{\text{tx}} \cdot N_{\text{tz}}$ and $N_{\text{r}} = N_{\text{rx}} \cdot N_{\text{rz}}$, the base-station and each user are assumed to have $M_{\text{t}} \leq N_{\text{t}}$ and $M_{\text{r}} \leq N_{\text{r}}$ RF chains, respectively.

For the channel $\mathbf{H}_k \in \mathbb{C}^{N_{\text{r}} \times N_{\text{t}}}$ between the base-station and the k -th user (where $k = 1, \dots, K_{\text{cell}}$), we assume an extended geometric propagation model over L_k clusters/paths [6],

[46]

$$\mathbf{H}_k = \sqrt{\frac{N_r N_t}{L_k}} \sum_{\ell=1}^{L_k} \alpha_{k,\ell} \mathbf{u}_{k,\ell} \mathbf{v}_{k,\ell}^\dagger. \quad (1)$$

In (1), $\alpha_{k,\ell}$, $\mathbf{u}_{k,\ell}$ and $\mathbf{v}_{k,\ell}$ denote the complex gain, the array steering vector at the user end corresponding to the angle of arrival (AoA) in azimuth/zenith, and the array steering vector at the base-station corresponding to the angle of departure (AoD) in azimuth/zenith, respectively. The cluster gains are assumed to be independent and identically distributed (i.i.d.) standard complex Gaussian random variables: $\alpha_{k,\ell} \sim \mathcal{CN}(0, 1)$. The normalization of the channel ensures that $\mathcal{E} [\text{Tr}(\mathbf{H}_k \mathbf{H}_k^\dagger)] = N_r N_t$.

In terms of the system model, we focus on the narrowband aspects and assume that the base-station serves $K \leq K_{\text{cell}}$ users simultaneously with data along M_t RF chains. The base-station precodes r_m data-streams for the m -th user with the $r_m \times 1$ symbol vector \mathbf{s}_m using the $M_t \times r_m$ digital/baseband precoder $\mathbf{F}_{\text{Dig}, m}$ which is then up-converted to the carrier frequency by the use of the $N_t \times M_t$ RF precoder \mathbf{F}_{RF} . This results in the following system equation at the k -th user

$$\mathbf{y}_k = \sqrt{\frac{\rho}{K}} \mathbf{H}_k \mathbf{F}_{\text{RF}} \cdot \left[\sum_{m=1}^K \mathbf{F}_{\text{Dig}, m} \mathbf{s}_m \right] + \mathbf{n}_k \quad (2)$$

where ρ is the pre-precoding SNR and $\mathbf{n}_k \sim \mathcal{CN}(\mathbf{0}, \mathbf{I}_{N_r})$ is the $N_r \times 1$ white Gaussian noise vector added at the k -th user. We assume that \mathbf{s}_m are i.i.d. complex Gaussian random vectors with $\mathcal{E}[\mathbf{s}_m] = \mathbf{0}$ and $\mathcal{E}[\mathbf{s}_m \mathbf{s}_m^\dagger] = \mathbf{I}_{r_m}$.

At the k -th user, we assume that \mathbf{y}_k is processed (down-converted) with an $N_r \times M_r$ user-specific RF combiner $\mathbf{G}_{\text{RF}, k}$ followed by a user-specific $M_r \times r_k$ digital combiner $\mathbf{G}_{\text{Dig}, k}$ to produce an estimate of \mathbf{s}_k as follows

$$\hat{\mathbf{s}}_k = \mathbf{G}_{\text{Dig}, k}^\dagger \mathbf{G}_{\text{RF}, k}^\dagger \mathbf{y}_k \quad (3)$$

$$= \sqrt{\frac{\rho}{K}} \mathbf{G}_{\text{Dig}, k}^\dagger \mathbf{G}_{\text{RF}, k}^\dagger \mathbf{H}_k \mathbf{F}_{\text{RF}} \mathbf{F}_{\text{Dig}, k} \mathbf{s}_k + \sqrt{\frac{\rho}{K}} \mathbf{G}_{\text{Dig}, k}^\dagger \mathbf{G}_{\text{RF}, k}^\dagger \mathbf{H}_k \mathbf{F}_{\text{RF}} \sum_{m=1, m \neq k}^K \mathbf{F}_{\text{Dig}, m} \mathbf{s}_m + \mathbf{n}_k. \quad (4)$$

The achievable rate \mathcal{R}_k (in nats/s/Hz) at the k -th user when treating multi-user interference as noise is given as

$$\mathcal{R}_k = \log \det \left(\mathbf{I}_{r_k} + \frac{\rho}{K} \mathbf{G}_{\text{Dig}, k}^\dagger \mathbf{G}_{\text{RF}, k}^\dagger \mathbf{H}_k \mathbf{F}_{\text{RF}} \mathbf{F}_{\text{Dig}, k} \mathbf{F}_{\text{Dig}, k}^\dagger \mathbf{F}_{\text{RF}}^\dagger \mathbf{H}_k^\dagger \mathbf{G}_{\text{RF}, k} \mathbf{G}_{\text{Dig}, k} \cdot \Sigma_{\text{intf}}^{-1} \right) \quad (5)$$

where Σ_{intf} denotes the interference and noise covariance matrix

$$\Sigma_{\text{intf}} = \mathbf{I}_{r_k} + \frac{\rho}{K} \mathbf{G}_{\text{Dig}, k}^\dagger \mathbf{G}_{\text{RF}, k}^\dagger \mathbf{H}_k \mathbf{F}_{\text{RF}} \left(\sum_{m \neq k} \mathbf{F}_{\text{Dig}, m} \mathbf{F}_{\text{Dig}, m}^\dagger \right) \mathbf{F}_{\text{RF}}^\dagger \mathbf{H}_k^\dagger \mathbf{G}_{\text{RF}, k} \mathbf{G}_{\text{Dig}, k}. \quad (6)$$

The traditional use of *finite-rate feedback* has been to convey the index of a precoder matrix from an appropriately-designed codebook of precoders to assist with adaptive transmissions to improve \mathcal{R}_k [47], [48]. More generally, feedback from users can also be used to aid in scheduling, channel estimation and advanced/non-codebook based precoder design. In this work, as we will see later in Sec. III, we assume that each user feeds back its top beam indices, an estimate of the received SNR and signal phase, and cross-correlation of the top receive beams to assist with the design of a non-codebook based multi-user precoder structure. In terms of precoder constraints, we make the assumption that $\mathbf{F}_{\text{Dig}, m} \in \mathbb{C}^{M_t \times r_m}$.

For the RF precoder, we assume that the amplitude and phase of each entry in \mathbf{F}_{RF} are controlled by a finite precision gain controller and phase shifter, respectively. In other words, the amplitude and phase come from a set of $2^{B_{\text{amp}}}$ and $2^{B_{\text{phase}}}$ quantization levels

$$|\mathbf{F}_{\text{RF}}(i, j)| \in \{A_1, \dots, A_{2^{B_{\text{amp}}}}\}, \quad \angle \mathbf{F}_{\text{RF}}(i, j) \in \{\phi_1, \dots, \phi_{2^{B_{\text{phase}}}}\}, \quad (7)$$

where $0 \leq A_1 < A_2 < \dots < A_{2^{B_{\text{amp}}}}$. Prior work on hybrid beamforming such as [17], [30]–[32] etc., assume that the RF precoder can only be controlled by a phase shifter. However, such constraining assumptions are not reflective of practical implementations [38]–[40], where an independent gain controller can be used in every RF chain for every antenna. With these structural constraints on the precoder, the transmit power constraint is captured by

$$\sum_{m=1}^K \text{Tr} \left(\mathbf{F}_{\text{Dig}, m}^\dagger \mathbf{F}_{\text{RF}}^\dagger \mathbf{F}_{\text{RF}} \mathbf{F}_{\text{Dig}, m} \right) \leq K. \quad (8)$$

We are interested in the design of RF and digital precoders with the sum rate, $\mathcal{R}_{\text{sum}} \triangleq \sum_{k=1}^K \mathcal{R}_k$, being the metric to maximize. In general, we only need the constraints $\sum_{k=1}^K r_k \leq M_t \leq N_t$ and $\max_k r_k \leq M_r \leq N_r$. However, the considered sum rate optimization with such an assumption is quite complicated. To overcome this complexity, we consider a simple use-case in this work.

III. MULTI-USER BEAMFORMER DESIGN

We are interested in the practically-motivated setting where each user is equipped with only one RF chain and the base-station transmits one data-stream to each user that is simultaneously scheduled. In this scenario, $M_r = r_k = 1$ (for all $k = 1, \dots, K$) and $M_t = K \leq N_t$. The system

decoding model in (2) and (4) reduce to

$$\hat{\mathbf{s}}_k = \mathbf{G}_{\text{Dig},k}^\dagger \mathbf{G}_{\text{RF},k}^\dagger \mathbf{y}_k = \underbrace{\mathbf{G}_{\text{Dig},k}^\dagger}_{1 \times 1} \underbrace{\mathbf{G}_{\text{RF},k}^\dagger}_{1 \times N_r} \cdot \left(\sqrt{\frac{\rho}{K}} \mathbf{H}_k \underbrace{\mathbf{F}_{\text{RF}}}_{N_t \times K} \cdot \underbrace{\mathbf{F}_{\text{Dig}}}_{K \times K} \cdot \underbrace{\mathbf{s}}_{K \times 1} + \mathbf{n}_k \right) \quad (9)$$

$$= \sqrt{\frac{\rho}{K}} \cdot \mathbf{g}_k^\dagger \mathbf{H}_k [\mathbf{f}_1 \mathbf{s}_1, \dots, \mathbf{f}_K \mathbf{s}_K] + \mathbf{g}_k^\dagger \mathbf{n}_k \quad (10)$$

where $\mathbf{F}_{\text{Dig}} = [\mathbf{F}_{\text{Dig},1}, \dots, \mathbf{F}_{\text{Dig},K}]$ and $\mathbf{s} = [\mathbf{s}_1, \dots, \mathbf{s}_K]^\top$, and the second equation follows assuming⁴ $\mathbf{f}_k = \mathbf{F}_{\text{RF}} \mathbf{F}_{\text{Dig},k}$ and $\mathbf{G}_{\text{RF},k} = \mathbf{g}_k$. The power constraint is equivalent to $\sum_{m=1}^K \mathbf{f}_k^\dagger \mathbf{f}_k \leq K$ and \mathcal{R}_k reduces to

$$\mathcal{R}_k = \log \left(1 + \frac{\frac{\rho}{K} \cdot |\mathbf{g}_k^\dagger \mathbf{H}_k \mathbf{f}_k|^2}{1 + \frac{\rho}{K} \cdot \sum_{m \neq k} |\mathbf{g}_k^\dagger \mathbf{H}_k \mathbf{f}_m|^2} \right). \quad (11)$$

The focus of this section is to first develop an advanced feedback mechanism and a systematic design of the multi-user beamforming structure based on a directional representation of the channel. This structure allows the base-station to combat multi-user interference in simultaneous transmissions.

A. Initial Beam Alignment

Enabling multi-user transmissions in practice is critically dependent on an initial beam acquisition process (commonly known as the *beam alignment* phase). In a practical implementation such as 3GPP 5G-NR, beam alignment corresponds to a beam sweep over a block of secondary synchronization (SS) signals transmitted over multiple ports/RF chains. The use of multiple directional beams over multiple ports results in a composite beam pattern at the base-station end (as seen from the user side). The composite pattern can lead to uncertainty in the direction of the strongest path between the base-station and the user. This directional ambiguity is subsequently resolved with a beam refinement over the individual constituent beams that make the composite beam on separate resource elements. Beam refinement allows identification and ambiguity resolution of the constituent beams.

⁴A simple realization of the hybrid precoding architecture is achieved by setting $\mathbf{F}_{\text{Dig}} = \mathbf{I}_K$ and the desired \mathbf{f}_k for the k -th user is set as the k -th column of \mathbf{F}_{RF} . The desired \mathbf{f}_k is such that $\mathbf{f}_k^\dagger \mathbf{f}_k \leq 1$ and meets the quantization constraints in (7). In a practical implementation, \mathbf{F}_{Dig} could be primarily used for sub-band precoding and in the narrowband context of this work, $\mathbf{F}_{\text{Dig}} = \mathbf{I}_K$ would reflect such an implementation-driven model.

Such a “post directional ambiguity resolved” beam alignment process is modeled by assuming that the base-station is equipped with an N element codebook \mathcal{F}_{tr}

$$\mathcal{F}_{\text{tr}} = \left\{ \mathbf{f}_{\text{tr},1}, \dots, \mathbf{f}_{\text{tr},N} \right\}, \quad (12)$$

and the k -th user is equipped with an M element user-specific codebook $\mathcal{G}_{\text{tr}}^k$

$$\mathcal{G}_{\text{tr}}^k = \left\{ \mathbf{g}_{\text{tr},1}^{(k)}, \dots, \mathbf{g}_{\text{tr},M}^{(k)} \right\}. \quad (13)$$

A typical design methodology for \mathcal{F}_{tr} is a hierarchical design with different sets of beams that trade-off peak array gain at the cost of initial beam acquisition latency. For example, at least from the 3GPP 5G-NR perspective, the designs of \mathcal{F}_{tr} and $\mathcal{G}_{\text{tr}}^k$ are intended to be implementation-specific at the base-station and user ends, respectively. Nevertheless, overarching design guidelines for beam broadening are provided in [14], [19], [49], [50]. In particular, a broadened beam can be generated by an optimal co-phasing of a number of array steering vectors in appropriately chosen directions. Both the number of such vectors as well as their steering directions can be optimized to produce a broadened beam. It must also be pointed out that most of the beam broadening works have some variations in terms of design principles and these variations themselves do not affect the flavor of results reported in this paper.

In the beam alignment phase, the top- P beam indices at the base-station and each user that maximize an estimate of the received SNR are learned. In particular, the received SNR corresponding to the (m, n) -th beam index pair at the k -th user is given as

$$\text{SNR}_{\text{rx}}^{(k)}(m, n) = \left| \left(\mathbf{g}_{\text{tr},m}^{(k)} \right)^\dagger \mathbf{H}_k \mathbf{f}_{\text{tr},n} \right|^2. \quad (14)$$

Let the beam pair indices at the k -th user be arranged in non-increasing order of the received SNR and let the top- P beam pair indices be denoted as

$$\mathcal{M} = \left\{ (m_1^k, n_1^k), \dots, (m_P^k, n_P^k) \right\}. \quad (15)$$

With the simplified notation of

$$\text{SNR}_{\text{rx},\ell}^{(k)} \triangleq \text{SNR}_{\text{rx}}^{(k)}(m_\ell^k, n_\ell^k), \quad \ell = 1, \dots, P, \quad (16)$$

we have $\text{SNR}_{\text{rx},1}^{(k)} \geq \dots \geq \text{SNR}_{\text{rx},P}^{(k)}$. With the initial beam alignment methodology as described above, we now leverage the top- P beam information learned at the k -th user to estimate the channel matrix \mathbf{H}_k and to design \mathbf{F}_{RF} at the base-station end.

B. Channel Reconstruction and Beamformer Design

A typical use of the feedback information at the base-station is to select the top/best beam indices for all the users and to leverage this information to construct a multi-user transmission scheme. Such an approach is adopted in [24], where multi-user beam designs leveraging only the top beam pair index, (m_1^k, n_1^k) , and intended to serve different objectives are proposed: i) greedily (from each user's perspective) steering a beam to the best direction for that user (called the *beam steering* scheme), ii) using the information collated from different users to combat interference to other simultaneously scheduled users via a zeroforcing solution (called the *zeroforcing* scheme), and iii) for leveraging both the beam steering and interference management objectives via a generalized eigenvector optimization (called the *generalized eigenvector* scheme). If the beam pair (m_1^k, n_1^k) is blocked or fades, the k -th user requests the base-station to switch to the beam index n_2^k and it switches to the beam with index m_2^k (and so on) [10].

In this work, we propose to generalize the structures in [24] by leveraging *all* the top- P beam pair indices fed back from each user. In this direction, the base-station intends to *reconstruct* or *estimate* a rank- P approximation of (a scaled version of) the channel matrix \mathbf{H}_k corresponding to the k -th user as follows

$$\hat{\mathbf{H}}_k = \sum_{\ell=1}^P \hat{\alpha}_{k,\ell} \hat{\mathbf{u}}_{k,\ell} \hat{\mathbf{v}}_{k,\ell}^\dagger, \quad (17)$$

where $\hat{\mathbf{u}}_{k,\ell}$ and $\hat{\mathbf{v}}_{k,\ell}$ are defined as estimates of the array steering vectors $\mathbf{u}_{k,\ell}$ and $\mathbf{v}_{k,\ell}$, respectively. Given the channel model structure in (1), (17) is simplified by estimating $\mathbf{v}_{k,\ell}$ and $|\alpha_{k,\ell}|$ by $\mathbf{f}_{\text{tr},n_\ell^k}$ and $\gamma_{k,\ell}$, respectively, where

$$\gamma_{k,\ell} \triangleq \sqrt{\mathcal{Q}_{B_{\text{SNR}}}(\text{SNR}_{\text{rx},\ell}^{(k)})} \quad (18)$$

for some choice of B_{SNR} . In the above description, $\mathcal{Q}_B(\cdot)$ denotes an appropriately-defined B -bit quantization operation⁵ of the quantity under consideration. However, estimating $\hat{\mathbf{H}}_k$ as in (17) is not complete until we have an estimate for $\angle\alpha_{k,\ell}$ and $\mathbf{u}_{k,\ell}$. The quantity $\angle\alpha_{k,\ell}$ can be estimated by the user with the same reference symbol resource (or pilot symbol) transmitted during the beam training phase with no additional training overhead. Therefore, we define $\varphi_{k,\ell}$ as the $B_{\text{est, phase}}$ -bit quantization of the phase of an estimate $\hat{\mathbf{s}}_{\text{tr},k,\ell}$ of the pilot symbol $\mathbf{s}_{\text{tr},k,\ell}$

$$\varphi_{k,\ell} \triangleq \mathcal{Q}_{B_{\text{est, phase}}}(\angle\hat{\mathbf{s}}_{\text{tr},k,\ell}), \quad \text{where } \hat{\mathbf{s}}_{\text{tr},k,\ell} = \left(\mathbf{g}_{\text{tr},m_\ell^k}^{(k)}\right)^\dagger \left[\sqrt{\rho}\mathbf{H}_k\mathbf{f}_{\text{tr},n_\ell^k}\mathbf{s}_{\text{tr},k,\ell} + \mathbf{n}_{k,\ell}\right] \quad (19)$$

⁵A B -bit quantization operation is precisely specified if 2^B disjoint intervals that exactly and entirely span the range of the quantity and a representative/quantized value from each interval are specified.

for some choice of $B_{\text{est, phase}}$. The noise term $\mathbf{n}_{k,\ell}$ captures the additive noise in the initial beam alignment process corresponding to the top- P beam pairs.

For $\mathbf{u}_{k,\ell}$, we note that the base-station not only needs the beam indices $\{m_\ell^k\}$ that are useful for the user side, but also the useful part of the user's codebook ($\mathcal{G}_{\text{tr}}^k$) since the base-station is typically unaware of it. To avoid this unnecessary complexity and feedback given the proprietary structure of $\mathcal{G}_{\text{tr}}^k$, we assume that the k -th user uses a multi-user reception beam \mathbf{g}_k . In the simplest manifestation, \mathbf{g}_k could be the best training beam learned in the beam alignment phase, $\mathbf{g}_{\text{tr}, m_1^k}^{(k)}$. However, a more sophisticated choice for \mathbf{g}_k is not precluded. For example, an iterative choice that maximizes the SINR (instead of the SNR) could be considered for \mathbf{g}_k .

We then note that the estimated SINR, defined as,

$$\widehat{\text{SINR}}_k \triangleq \frac{\frac{\rho}{K} \cdot |\mathbf{g}_k^\dagger \widehat{\mathbf{H}}_k \mathbf{f}_k|^2}{1 + \frac{\rho}{K} \cdot \sum_{m \neq k} |\mathbf{g}_k^\dagger \widehat{\mathbf{H}}_k \mathbf{f}_m|^2} \quad (20)$$

is only dependent on $\widehat{\mathbf{H}}_k$ in the form of $\mathbf{g}_k^\dagger \widehat{\mathbf{H}}_k$. Building on this fact, each user generates $\{\beta_{k,\ell}\}$, defined as,

$$\beta_{k,\ell} \triangleq \mathbf{g}_k^\dagger \widehat{\mathbf{u}}_{k,\ell} \text{ where } \widehat{\mathbf{u}}_{k,\ell} = \mathbf{g}_{\text{tr}, m_\ell^k}^{(k)}. \quad (21)$$

It then quantizes the amplitude and phase of $\beta_{k,\ell}$ for some choice of $B_{\text{corr, amp}}$ and $B_{\text{corr, phase}}$ and feeds them back

$$\mu_{k,\ell} \triangleq \mathcal{Q}_{B_{\text{corr, amp}}}(|\beta_{k,\ell}|), \quad \nu_{k,\ell} \triangleq \mathcal{Q}_{B_{\text{corr, phase}}}(\angle \beta_{k,\ell}). \quad (22)$$

For both $\varphi_{k,\ell}$ and $\nu_{k,\ell}$, without loss in generality, relative phases with respect to $\varphi_{k,1}$ and $\nu_{k,1}$ (that is, $\varphi_{k,\ell} - \varphi_{k,1}$ and $\nu_{k,\ell} - \nu_{k,1}$) can be reported.

The mappings between the quantities of interest and the approximated quantities as well as the feedback overhead needed from each user to implement the proposed scheme are described in Table I. While the feedback overhead increases linearly with P (the rank of the channel approximation), there are diminishing returns in terms of channel representation accuracy since the clusters captured in $\widehat{\mathbf{H}}_k$ are sub-dominant as P increases (and are eventually limited by L_k). Thus, it is useful to select P to trade-off these two conflicting objectives.

Following the above discussion, the k -th user feeds back the $P \times 5$ matrix \mathbf{P}_k , defined as

$$\mathbf{P}_k \triangleq \begin{bmatrix} n_1^k & \gamma_{k,1} & 0 & \mu_{k,1} & 0 \\ n_2^k & \gamma_{k,2} & \varphi_{k,2} - \varphi_{k,1} & \mu_{k,2} & \nu_{k,2} - \nu_{k,1} \\ \vdots & \vdots & \vdots & \vdots & \vdots \\ n_P^k & \gamma_{k,P} & \varphi_{k,P} - \varphi_{k,1} & \mu_{k,P} & \nu_{k,P} - \nu_{k,1} \end{bmatrix}, \quad (23)$$

TABLE I: Mappings between quantities describing \mathbf{H}_k and the approximated quantities, and their feedback overhead.

Quantity of Interest	Approximated Quantity	Feedback Overhead
Array steering vector at base-station end ($\mathbf{v}_{k,\ell}$)	Base-station beam indices (n_ℓ^k)	$P \cdot \log_2(N)$
Gain of cluster coefficient ($ \alpha_{k,\ell} $)	Received SNR in beam alignment ($\text{SNR}_{\text{rx},\ell}^{(k)}$)	$P \cdot B_{\text{SNR}}$
Phase of cluster coefficient ($\angle \alpha_{k,\ell}$)	Estimated phase in beam alignment ($\angle \hat{\mathbf{s}}_{\text{tr},k,\ell}$)	$(P-1) \cdot B_{\text{est, phase}}$
Array steering vector at user end ($\mathbf{u}_{k,\ell}$)	Amplitude of codebook correlation ($ \beta_{k,\ell} $)	$P \cdot B_{\text{corr, amp}}$
	Phase of codebook correlation ($\angle \beta_{k,\ell}$)	$(P-1) \cdot B_{\text{corr, phase}}$

and the base-station approximates $\mathbf{g}_k^\dagger \hat{\mathbf{H}}_k$ as follows

$$\mathbf{g}_k^\dagger \hat{\mathbf{H}}_k = \sum_{\ell=1}^P \mu_{k,\ell} \gamma_{k,\ell} \cdot e^{j(\varphi_{k,\ell} + \nu_{k,\ell})} \cdot \left(\mathbf{f}_{\text{tr}, n_\ell^k} \right)^\dagger. \quad (24)$$

In other words, $\mathbf{g}_k^\dagger \hat{\mathbf{H}}_k$ is represented as a linear combination of the top- P beams as estimated from \mathcal{F}_{tr} in the initial beam alignment phase. The weights in this linear combination correspond to the relative strengths of the clusters as distinguished by the codebook resolution (at both ends).

The base-station uses the channel matrix constructed for each user based on its feedback information ($\mathbf{g}_k^\dagger \hat{\mathbf{H}}_k$) and generates a good beamformer structure, illustrated in the next result, for use in multi-user transmissions.

Proposition 1. *The zeroforcing beamformer structure is one where for every user that is simultaneously scheduled, the beam \mathbf{f}_k nulls the multi-user interference in $\widehat{\text{SINR}}_m$, $m \neq k$ with $\widehat{\text{SINR}}_m$ as given in (20). The beams $\{\mathbf{f}_m\}$ in the zeroforcing structure are the unit-norm column vectors of the $N_t \times K$ matrix $\mathcal{H}^\dagger (\mathcal{H} \mathcal{H}^\dagger)^{-1}$, where \mathcal{H} is the $K \times N_t$ matrix given as*

$$\mathcal{H} = \begin{bmatrix} \mathbf{g}_1^\dagger \hat{\mathbf{H}}_1 \\ \mathbf{g}_2^\dagger \hat{\mathbf{H}}_2 \\ \vdots \\ \mathbf{g}_K^\dagger \hat{\mathbf{H}}_K \end{bmatrix} = \begin{bmatrix} \sum_{\ell=1}^P \mu_{1,\ell} \gamma_{1,\ell} \cdot e^{j(\varphi_{1,\ell} + \nu_{1,\ell})} \cdot \left(\mathbf{f}_{\text{tr}, n_\ell^1} \right)^\dagger \\ \sum_{\ell=1}^P \mu_{2,\ell} \gamma_{2,\ell} \cdot e^{j(\varphi_{2,\ell} + \nu_{2,\ell})} \cdot \left(\mathbf{f}_{\text{tr}, n_\ell^2} \right)^\dagger \\ \vdots \\ \sum_{\ell=1}^P \mu_{K,\ell} \gamma_{K,\ell} \cdot e^{j(\varphi_{K,\ell} + \nu_{K,\ell})} \cdot \left(\mathbf{f}_{\text{tr}, n_\ell^K} \right)^\dagger \end{bmatrix}. \quad (25)$$

Proof. See Appendices A and B. □

IV. UPPER BOUNDS FOR \mathcal{R}_{sum}

We are interested in benchmarking the performance of the zeroforcing structure against an upper bound on \mathcal{R}_{sum} . The goal of optimizing \mathcal{R}_{sum} over $\{\mathbf{f}_k, \mathbf{g}_k\}$ with perfect channel state information $\{\mathbf{H}_k\}$ is a non-convex optimization problem [42]–[44] that appears to be complicated. In this context, an alternate formulation based on the signal-to-leakage and noise ratio metric [45] that *simultaneously* maximizes the array gain seen by the k -th user, $|\mathbf{g}_k^\dagger \mathbf{H}_k \mathbf{f}_k|^2$, and minimizes the interfering array gain seen by the other users, $|\mathbf{g}_m^\dagger \mathbf{H}_m \mathbf{f}_k|^2$, $m \neq k$ is relevant. Since these objectives are in some sense conflicting and can be weighed differently, we consider the composite metric

$$\text{SLNR}_k \triangleq \frac{\eta_{k,k} |\mathbf{g}_k^\dagger \mathbf{H}_k \mathbf{f}_k|^2}{1 + \sum_{m \neq k} \eta_{m,k} |\mathbf{g}_m^\dagger \mathbf{H}_m \mathbf{f}_k|^2} \quad (26)$$

for an appropriate set of weighting factors $\eta_{m,k} \geq 0$ with $m, k \in \{1, \dots, K\}$.

A. Upper Bound Motivated by the Zeroforcing Structure

Building on Prop. 1, we now develop an upper bound for \mathcal{R}_{sum} motivated by the zeroforcing structure. In this direction, we consider a signal-to-leakage-type metric equivalent of (26) based on the estimated channel matrix $\hat{\mathbf{H}}_k$

$$\widehat{\text{SLNR}}_k \triangleq \frac{\eta_{k,k} |\mathbf{g}_k^\dagger \hat{\mathbf{H}}_k \mathbf{f}_k|^2}{1 + \sum_{m \neq k} \eta_{m,k} |\mathbf{g}_m^\dagger \hat{\mathbf{H}}_m \mathbf{f}_k|^2} \quad (27)$$

for an appropriate set of weighting factors $\eta_{m,k} \geq 0$ with $m, k \in \{1, \dots, K\}$.

Proposition 2. *Assuming that $\{\hat{\mathbf{H}}_m^\dagger \mathbf{g}_m\}$ and $\{\eta_{m,k}\}$ are known at the base-station, the choice of \mathbf{f}_k that maximizes $\widehat{\text{SLNR}}_k$ is given by the generalized eigenvector structure*

$$\mathbf{f}_k = \frac{\left(\mathbf{I}_{N_t} + \sum_{m \neq k} \eta_{m,k} \hat{\mathbf{H}}_m^\dagger \mathbf{g}_m \mathbf{g}_m^\dagger \hat{\mathbf{H}}_m \right)^{-1} \hat{\mathbf{H}}_k^\dagger \mathbf{g}_k}{\left\| \left(\mathbf{I}_{N_t} + \sum_{m \neq k} \eta_{m,k} \hat{\mathbf{H}}_m^\dagger \mathbf{g}_m \mathbf{g}_m^\dagger \hat{\mathbf{H}}_m \right)^{-1} \hat{\mathbf{H}}_k^\dagger \mathbf{g}_k \right\|}. \quad (28)$$

Proof. See Appendix C. □

Several remarks are in order at this stage.

- In the case where $\eta_{m,k}$ are set to zero for all $m \neq k$ (that is, the focus is *not* on interference management), the solution in (28) reduces to

$$\mathbf{f}_k = \frac{\hat{\mathbf{H}}_k^\dagger \mathbf{g}_k}{\|\hat{\mathbf{H}}_k^\dagger \mathbf{g}_k\|} = \frac{\sum_{\ell=1}^P \mu_{k,\ell} \gamma_{k,\ell} \cdot e^{-j(\varphi_{k,\ell} + \nu_{k,\ell})} \cdot \mathbf{f}_{\text{tr}, n_\ell^k}}{\left\| \sum_{\ell=1}^P \mu_{k,\ell} \gamma_{k,\ell} \cdot e^{-j(\varphi_{k,\ell} + \nu_{k,\ell})} \cdot \mathbf{f}_{\text{tr}, n_\ell^k} \right\|}. \quad (29)$$

This is not surprising, and the base-station *greedily* steers a beam along the weighted set of top- P beams from \mathcal{F}_{tr} for the k -th user. In other words, the base-station generates a set of transmit weights that are matched to the transmit angular spread of the channel as identified by the resolution of \mathcal{F}_{tr} .

- In the case where $\eta_{m,k} = 0$ except if $m = k$ or $m = m'$ (for a specific $m' \neq k$), it can be seen that \mathbf{f}_k reduces to

$$\mathbf{f}_k = \frac{\hat{\mathbf{H}}_k^\dagger \mathbf{g}_k - \eta_{m',k} \cdot \left(\mathbf{g}_{m'}^\dagger \hat{\mathbf{H}}_{m'} \hat{\mathbf{H}}_k^\dagger \mathbf{g}_k \right) \cdot \hat{\mathbf{H}}_{m'}^\dagger \mathbf{g}_{m'}}{\left\| \hat{\mathbf{H}}_k^\dagger \mathbf{g}_k - \eta_{m',k} \cdot \left(\mathbf{g}_{m'}^\dagger \hat{\mathbf{H}}_{m'} \hat{\mathbf{H}}_k^\dagger \mathbf{g}_k \right) \cdot \hat{\mathbf{H}}_{m'}^\dagger \mathbf{g}_{m'} \right\|}. \quad (30)$$

In other words, the specific design of \mathbf{f}_k in (30) removes a certain component of the beam corresponding to the m' -th user from the beam corresponding to the k -th user.

- In the general case, while it gets much harder to simplify \mathbf{f}_k in (28), it can be seen that \mathbf{f}_k has the structure

$$\mathbf{f}_k = \frac{\sum_{m=1}^K \hat{\delta}_{m,k} \hat{\mathbf{H}}_m^\dagger \mathbf{g}_m}{\left\| \sum_{m=1}^K \hat{\delta}_{m,k} \hat{\mathbf{H}}_m^\dagger \mathbf{g}_m \right\|} \quad (31)$$

for some complex scalars $\hat{\delta}_{m,k}$. In other words, the optimal \mathbf{f}_k is in the span of $\{\hat{\mathbf{H}}_m^\dagger \mathbf{g}_m\}$ with the weights $\{\hat{\delta}_{m,k}\}$ that make the linear combination being a complicated function of $\{\eta_{m,k}\}$ as well as $\{\hat{\mathbf{H}}_m^\dagger \mathbf{g}_m\}$.

- The above observations are not entirely surprising given the Karhunen-Loève interpretation of the eigen-space of the channel(s) [11], [51], [52] and utilizing an expansion of \mathbf{f}_k on this basis. Such an expansion is also consistent with Prop. 1 which shows that in the pure interference management case ($\eta_{m,k} \rightarrow \infty$ for all $m \neq k$), \mathbf{f}_k is given as

$$\mathbf{f}_k = \frac{\sum_{m=1}^K \mathcal{G}_{m,k} \hat{\mathbf{H}}_m^\dagger \mathbf{g}_m}{\left\| \sum_{m=1}^K \mathcal{G}_{m,k} \hat{\mathbf{H}}_m^\dagger \mathbf{g}_m \right\|} \quad (32)$$

where the $K \times K$ matrix $\mathcal{G} = (\mathcal{H}\mathcal{H}^\dagger)^{-1}$.

- On the other hand, from (24), we note that $\hat{\mathbf{H}}_m^\dagger \mathbf{g}_m$ is itself a linear combination of the beams from \mathcal{F}_{tr} . Thus, \mathbf{f}_k in (28) is a linear combination of beams from \mathcal{F}_{tr} . In other words, the design of \mathbf{f}_k is equivalent to a search over N scalar (complex) weights, where N denotes the size of the initial beam alignment codebook at the base-station end.

With this interpretation, while Prop. 2 considers only the maximization of $\widehat{\text{SLNR}}_k$ (not even the sum rate with $\hat{\mathbf{H}}_k$), we can consider the optimization of \mathcal{R}_{sum} over \mathbf{f}_k from a class \mathcal{F}_k ,

defined as

$$\mathcal{F}_k \triangleq \left\{ \mathbf{f}_k : \mathbf{f}_k = \frac{\sum_{n=1}^N \delta_{n,k} \mathbf{f}_{\text{tr},n}}{\left\| \sum_{n=1}^N \delta_{n,k} \mathbf{f}_{\text{tr},n} \right\|} \text{ such that } \delta_{n,k} \in \mathbb{C}, k = 1, \dots, K \right\}. \quad (33)$$

Theorem 1. Assume that the same multi-user beams \mathbf{g}_k as in the zeroforcing scheme are used for reception at the k -th user. Let $\{\delta_{n,k}^*\}$ be defined as the solution to the search over the complex scalars $\{\delta_{n,k}\}$

$$\{\delta_{n,k}^*\} = \arg \max_{\{\delta_{n,k} : \mathbf{f}_k \in \mathcal{F}_k\}} \mathcal{R}_{\text{sum}}. \quad (34)$$

With \mathbf{g}_k as above and

$$\mathbf{f}_k = \frac{\sum_{n=1}^N \delta_{n,k}^* \mathbf{f}_{\text{tr},n}}{\left\| \sum_{n=1}^N \delta_{n,k}^* \mathbf{f}_{\text{tr},n} \right\|}, \quad (35)$$

we obtain an upper bound to the sum rate with the zeroforcing scheme. \square

The proof is trivial following the structure of \mathbf{f}_k in the zeroforcing scheme in (32) and the definition of the class \mathcal{F}_k in (33). Since the structure in (35) is obtained as a search over scalar parameters, we call this upper bound a scalar optimization-based upper bound. Further, while (35) is difficult to practically implement, it provides a benchmark to compare the realizable zeroforcing scheme of Prop. 1.

Another important consequence of (35) is that the coefficients of \mathbf{f}_k for either the zeroforcing or the upper bound are (in general) not of equal amplitude. Thus, \mathbf{f}_k has to be quantized for implementation to ensure that the RF beamforming constraints are satisfied. In particular, we compute $\widehat{\mathbf{f}}_k$ with an appropriate quantization scheme as below

$$|\widehat{\mathbf{f}}_k(i)| = \widetilde{\mathcal{Q}}_{B_{\text{amp}}}(|\mathbf{f}_k(i)|), \quad \angle \widehat{\mathbf{f}}_k(i) = \widetilde{\mathcal{Q}}_{B_{\text{phase}}}(\angle \mathbf{f}_k(i)), \quad (36)$$

and use them in transmissions for the k -th user. Good choices for $\widetilde{\mathcal{Q}}(\cdot)$ will be discussed in Sec. V-C.

B. Bounding \mathcal{R}_{sum} with an Alternating/Iterative Optimization

We now propose an iterative maximization algorithm to optimize \mathcal{R}_{sum} over $\{\mathbf{f}_k, \mathbf{g}_k\}$. In this approach, we first optimize the SLNR metric over \mathbf{f}_k (assuming \mathbf{g}_k is fixed), and then optimize the SINR metric over \mathbf{g}_k (assuming \mathbf{f}_k is fixed). The algorithm is as follows:

- 1) Initialize $\{\mathbf{g}_k^{(1)}, k = 1, \dots, K\}$ randomly.

2) For $i = 1, \dots, N_{\text{stop}}$, where N_{stop} is chosen according to a stopping criterion to determine convergence:

- With $\{\mathbf{g}_k = \mathbf{g}_k^{(i)}, k = 1, \dots, K\}$ fixed, compute $\mathbf{f}_k^{(i)}$ as the solution to the following optimization

$$\mathbf{f}_k^{(i)} = \arg \max_{\mathbf{f}_k} \max_{\{\eta_{m,k}\}} \text{SLNR}_k. \quad (37)$$

From Lemma 1 in Appendix A, the solution to the above problem with $\{\eta_{m,k}\}$ fixed can be seen to be

$$\mathbf{f}_k = \frac{\left(\mathbf{I}_{N_t} + \sum_{m \neq k} \eta_{m,k} \mathbf{H}_m^\dagger \mathbf{g}_m^{(i)} \mathbf{g}_m^{(i)\dagger} \mathbf{H}_m \right)^{-1} \mathbf{H}_k^\dagger \mathbf{g}_k^{(i)}}{\left\| \left(\mathbf{I}_{N_t} + \sum_{m \neq k} \eta_{m,k} \mathbf{H}_m^\dagger \mathbf{g}_m^{(i)} \mathbf{g}_m^{(i)\dagger} \mathbf{H}_m \right)^{-1} \mathbf{H}_k^\dagger \mathbf{g}_k^{(i)} \right\|}. \quad (38)$$

This candidate \mathbf{f}_k has to be used to compute SLNR_k for all possible weights $\{\eta_{m,k}\}$ and optimized to produce $\{\mathbf{f}_k^{(i)}\}$.

- With $\{\mathbf{f}_k = \mathbf{f}_k^{(i)}, k = 1, \dots, K\}$ fixed, compute $\mathbf{g}_k^{(i+1)}$ as the solution to the following optimization

$$\mathbf{g}_k^{(i+1)} = \arg \max_{\mathbf{g}_k} \text{SINR}_k. \quad (39)$$

Again, from Lemma 1 in Appendix A, we have

$$\mathbf{g}_k^{(i+1)} = \left(\mathbf{I}_{N_r} + \frac{\rho}{K} \sum_{m \neq k} \mathbf{H}_k \mathbf{f}_m^{(i)} \mathbf{f}_m^{(i)\dagger} \mathbf{H}_k^\dagger \right)^{-1} \mathbf{H}_k \mathbf{f}_k^{(i)}. \quad (40)$$

3) Compute \mathcal{R}_{sum} with $\{\mathbf{f}_k^{(N_{\text{stop}})}\}$ and $\{\mathbf{g}_k^{(N_{\text{stop}}+1)}\}$ for a (potential) upper bound.

Numerical studies show that for almost all channel realizations, the proposed algorithm converges in a small number of steps ($N_{\text{stop}} \approx 10$) to lead to a tolerable level of difference between successive iterates of \mathcal{R}_{sum} . Further, while we are unable to theoretically establish that the proposed algorithm results in an upper bound to \mathcal{R}_{sum} , numerical studies (see Sec. V-D) suggest that it leads to an upper bound for almost all channel realizations.

V. NUMERICAL STUDIES

We now present numerical studies in a single-cell downlink framework to illustrate the advantages of the proposed beamforming solutions. The channel model from (1) is used to generate a channel matrix with $L_k = 6$ clusters, AoDs uniformly distributed in a $120^\circ \times 30^\circ$ coverage area, and AoAs uniformly distributed in a $120^\circ \times 120^\circ$ coverage area for each of the $k = 1, \dots, K_{\text{cell}}$ users in the cell. The AoD spread captures a traditional three-sector approach

with a 30° zenith coverage and the AoA spread corresponds to the assumption of the use of multiple subarrays [9] with the best subarray limited to a $120^\circ \times 120^\circ$ coverage. $L_k = 6$ is justified from millimeter wave channel measurements reported in [9], [12]. The antenna dimensions assumed in these studies are $N_{\text{tx}} = 16$ and $N_{\text{tz}} = 4$ at the base-station end, and $N_{\text{rx}} = 2$ and $N_{\text{rz}} = 2$ at each user. We consider simultaneous transmissions from the base-station to $K = 2$ out of the K_{cell} users in the cell.

In terms of user scheduling, commonly used criteria include a round robin or a proportionate fair scheduler. On the other hand, a recently proposed directional scheduler [24] leverages the smaller beamwidths afforded by large antenna dimensions to schedule users with dominant clusters that are spatially well-separated. In this work, the first of the $K = 2$ users is scheduled randomly and the second user is chosen to ensure that $\mathbf{f}_{\text{tr},n_1^2} \neq \mathbf{f}_{\text{tr},n_1^1}$. In other words, the considered scheduler implements a *directional avoidance* protocol with the dominant cluster in the channel of the first user separated spatially from the dominant cluster in the channel of the second user, as parsed by \mathcal{F}_{tr} . With this scheduler, we now primarily focus on the beamforming aspects.

For the initial beam alignment codebooks, based on the beam broadening principles proposed in [19], Figs. 1(a)-(d) illustrate the beam patterns in the azimuth plane for codebooks of sizes $N = 32$, $N = 16$, $N = 8$ and $N = 4$, respectively, to cover the $120^\circ \times 30^\circ$ AoD space with a 16×4 planar array at the base-station side. The optimization proposed in [19] results in a discrete Fourier transform (DFT) codebook solution for $N = 32$ and $N = 16$. From Fig. 1, we observe that a beam codebook of small size (e.g., $N = 4$) where each beam offers a broad directional coverage can reduce the acquisition latency at the cost of peak and/or worst-case array gain. On the other hand, a beam codebook of large size (e.g., $N = 32$) where each beam can offer precision in terms of beamspace (and array gain) comes at the cost of acquisition latency. For the codebooks at the user end, two codebook sizes ($M = 4$ for a reduced acquisition latency and $M = 16$ for performance improvement at the cost of acquisition latency) are considered with similar beam design principles as for the base-station side.

At this stage, it is worth noting that a number of system parameters impact the performance of the proposed multi-user schemes such as: i) Granularity of \mathcal{F}_{tr} and $\mathcal{G}_{\text{tr}}^k$ (initial beam alignment codebook sizes), ii) Coarseness of channel approximation (rank- P), iii) Finite-rate feedback of channel reconstruction parameters, and iv) Quantization of the resulting multi-user beams.

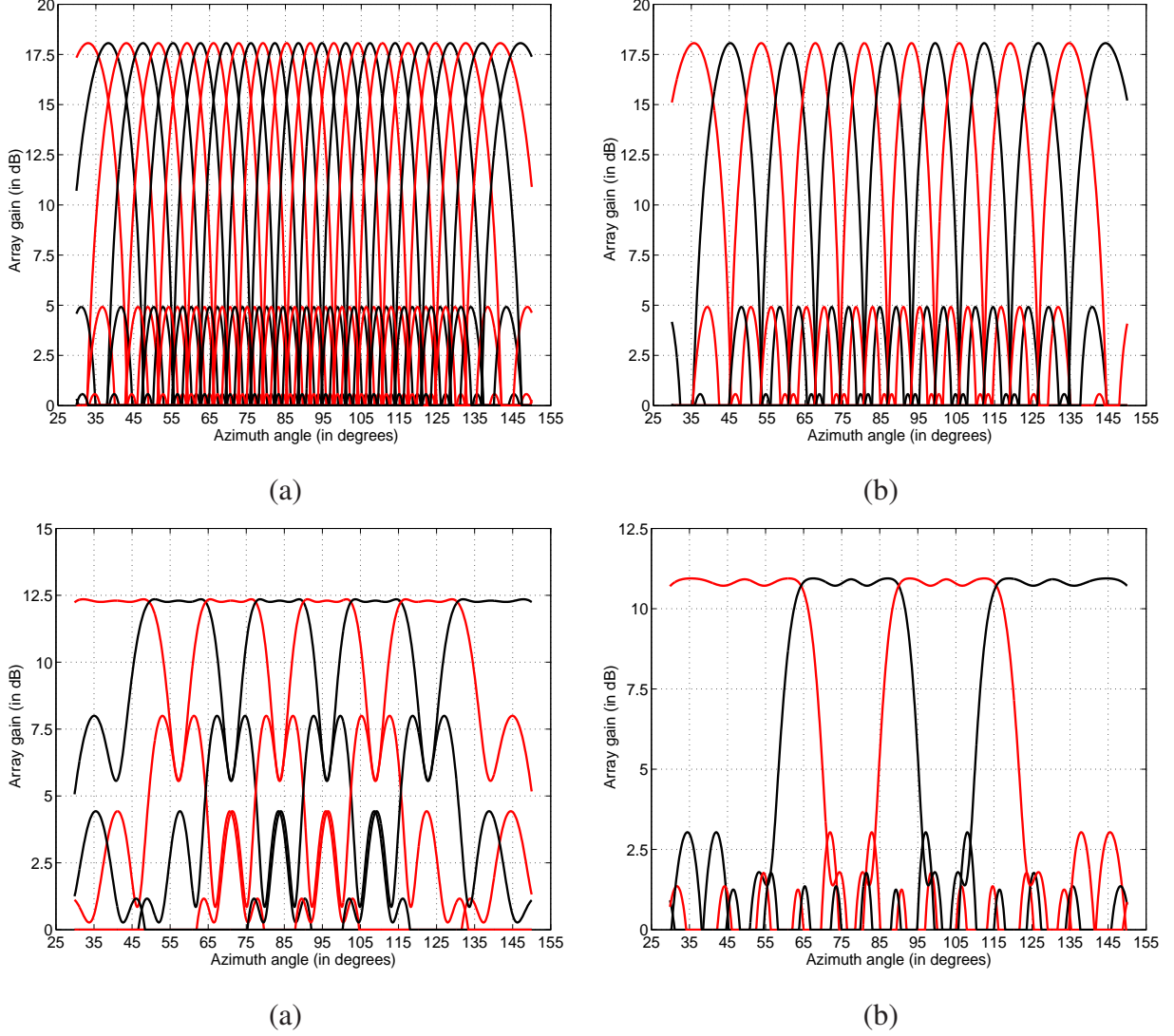


Fig. 1: Beam patterns in the azimuth plane of four different base-station codebooks, all covering a $120^\circ \times 30^\circ$ coverage area, with (a) $N = 32$, (b) $N = 16$, (c) $N = 8$, and (d) $N = 4$ elements in \mathcal{F}_{tr} .

A. Impact of Initial Beam Alignment Codebook

In the first study, we consider the relative performance of the zeroforcing scheme (proposed in Prop. 1) relative to a baseline beam steering scheme with different initial beam alignment codebooks. We assume that the system has infinite-precision feedback of channel reconstruction parameters and infinite-precision resolution in the quantization of multi-user beams. We also compare the performance of the proposed schemes with the zeroforcing scheme presented in [23],

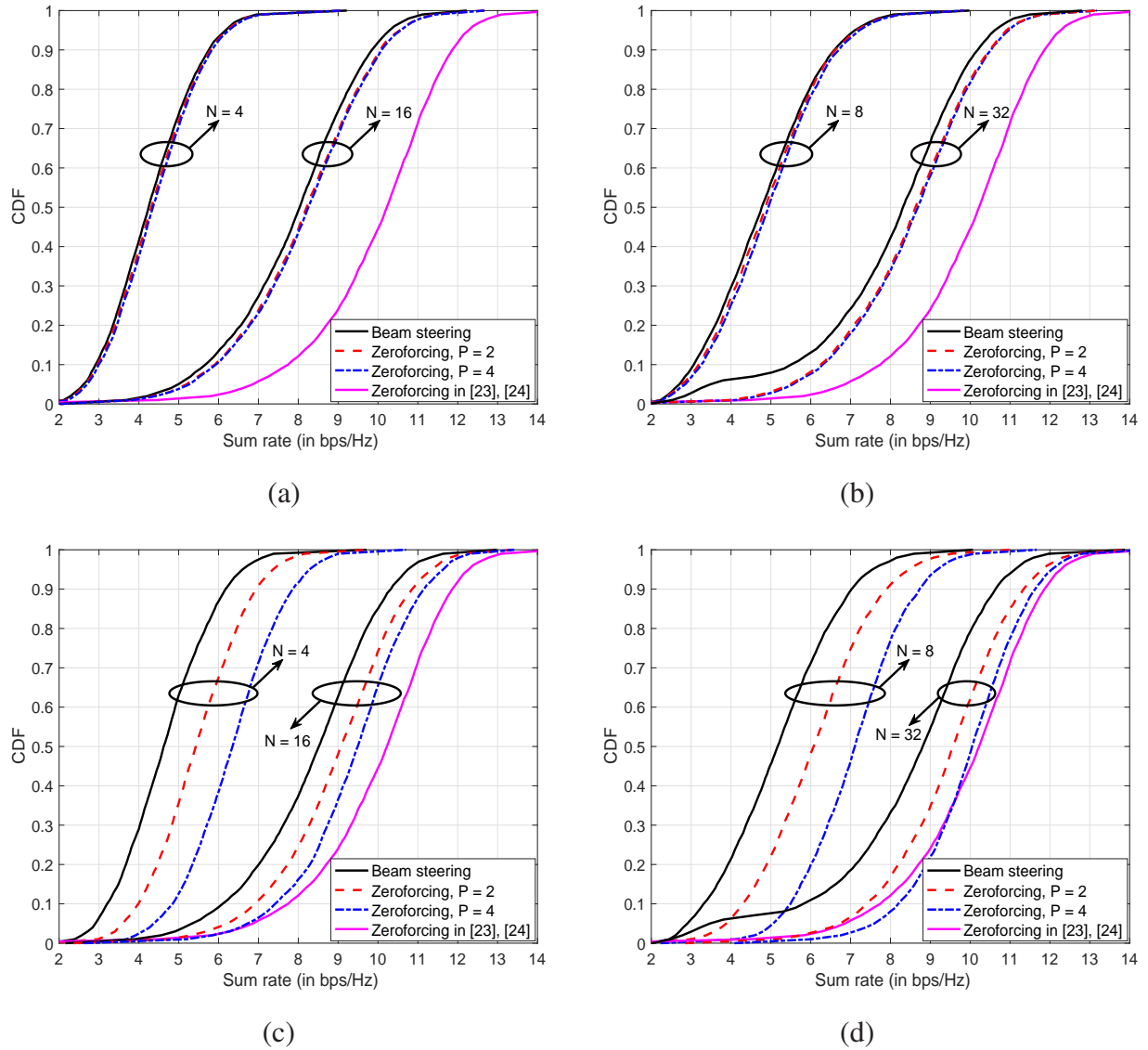


Fig. 2: CDF of sum rates for a beam steering scheme and the proposed zeroforcing scheme for different choices of N with $M = 4$ in (a) and (b), and $M = 16$ in (c) and (d).

[24], where the system is assumed to be able to find perfectly aligned directional beams in the training phase. Fig. 2 illustrates this comparative performance with different choices of P in approximating $\mathbf{g}_k^\dagger \hat{\mathbf{H}}_k$ and different codebook sizes (N and M).

While it is intuitive that there should be diminishing performance as P increases (since increasing P beyond the channel rank L_k is not expected to improve performance), whether this saturation in performance is observed with a low-rank channel approximation is dependent on the resolution of the codebooks. In particular, increasing P when the codebook granularity

is already poor (small M and N) does not lead to any performance improvement than observed with $P = 1$ (beam steering). On the other hand, with a high resolution for \mathcal{F}_{tr} (large N), even a rank-2 approximation appears to be sufficient to reap most of the performance improvement gains. This is because the performance of the baseline (beam steering) scheme is already quite good and significant relative improvement over it with increasing P has a lower likelihood unless the channel has a large number of similar gain clusters (a low-probability event). When M is large and N is small, the beam steering performance is poor and the channel can be better approximated with the higher codebook resolution of $\mathcal{G}_{\text{tr}}^k$ leading to a sustained performance improvement for even up to $P = 4$. For example, with $N = 4$ or 8 and $M = 16$, zeroforcing based on a rank-4 channel approximation leads to around 2 bps/Hz improvement at the median level.

In terms of performance comparison, note that the scheme from [23], [24] assumes $P = 1$ but infinite-precision in terms of beam alignment ($N = M \rightarrow \infty$). Thus, it is not surprising that as N and M increase, the performance of the proposed schemes compare well with that of [23], [24]. For lower codebook resolutions, the proposed schemes overcome the codebook disadvantage by leveraging a better channel approximation as P increases. These observations suggest that the optimal choice of the rank in approximating $\mathbf{g}_k^\dagger \hat{\mathbf{H}}_k$ (which in turn determines the feedback overhead) depends not only on the rank of the true channel \mathbf{H}_k , but also on the codebook granularities. In general, a higher P (and feedback overhead) is necessary if the codebook resolution is rich enough at the user end to allow the parsing of the channel better, but poor enough at the base-station end to allow a sustained performance improvement with increasing P . In particular, we provide the following heuristic design guidelines based on our studies

$$P = \begin{cases} 1 & \text{if } M \text{ and } N \text{ are small} \\ 2 & \text{if } M \text{ is small and } N \text{ is large} \\ 4 & \text{if } M \text{ is large.} \end{cases} \quad (41)$$

B. Quantizer Design

Towards the second study, we utilize different quantization functions to quantize the different parameters needed in channel reconstruction. For a phase term θ with a dynamic range of $[0, 2\pi)$ (e.g., $\angle \hat{\mathbf{s}}_{\text{tr},k,\ell}$ and $\angle \beta_{k,\ell}$), we use a uniform quantizer of the form

$$\mathcal{Q}_B(\theta) = \frac{2\pi}{2^B} \cdot \text{round} \left(\frac{2^B}{2\pi} \cdot \theta \right), \quad (42)$$

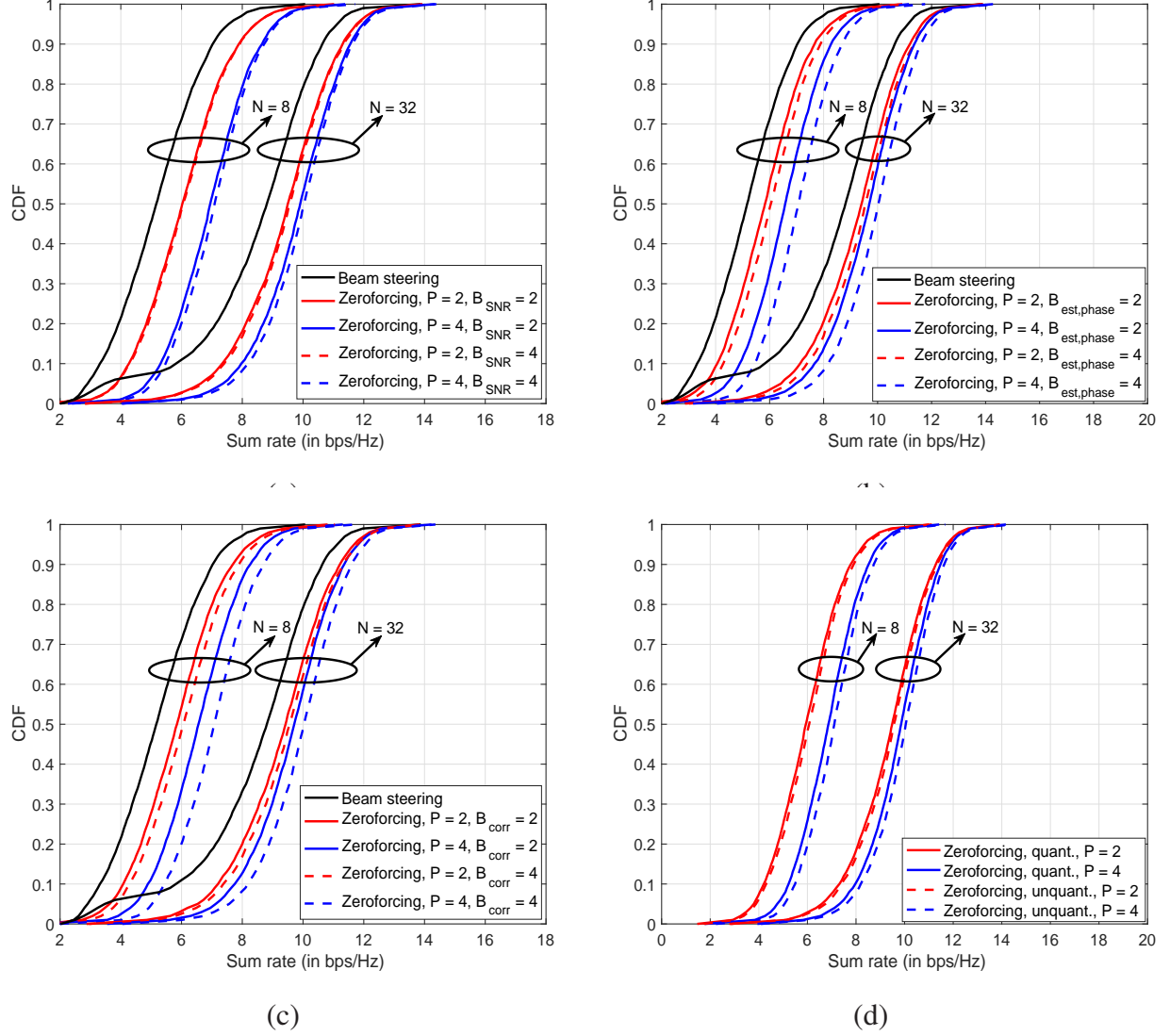


Fig. 3: CDF of sum rates of the different multi-user schemes with finite-rate feedback of (a) only received SNRs, (b) only received signal phases, (c) only user side cross-correlation information, and (d) all the parameters quantized simultaneously.

where $\text{round}(\cdot)$ stands for a function that rounds off the underlying quantity to the nearest integer. For an amplitude term α with a dynamic range of $[0, 1]$ (e.g., $|\beta_{k,\ell}|$), we use a non-uniform quantizer of the form

$$\mathcal{Q}_B(\alpha) = \frac{\text{round}((2^B - 1) \cdot \alpha)}{2^B - 1}. \quad (43)$$

The reason for scaling with respect to $2^B - 1$ in (43) instead of by 2^B is because we want the quantized set to include both 0 and 1 for proper cross-correlation quantization. For example, in

the typical case where the multi-user reception beam $\mathbf{g}_k = \mathbf{g}_{\text{tr}, m_1}^{(k)}$, we have $|\beta_{k,1}| = 1$ and the use of a uniform amplitude quantizer will not allow the correct reproduction of this important quantity at the base-station end.

Quantization of the SNR is performed on a dB scale rather than on a linear scale. This is intuitive since SNR measurements have a wide dynamic range. The proposed SNR quantizer is similar to quantizations considered in Fourth Generation (4G) systems. In particular, for a received SNR term ϱ (in dB) with a theoretically unbounded range (e.g., $10 \log_{10} (\text{SNR}_{\text{rx}, \ell}^{(k)})$), we first cap ϱ to a maximum value of ϱ_{\max} and quantize a spread of Δ (in dB) with 2^B quantization levels (denoted as ϱ_i) as follows:

$$\varrho_i = \varrho_{\max} - \frac{\Delta}{2^B - 1} \cdot i, \quad i = 0, \dots, 2^B - 1. \quad (44)$$

The quantization of ϱ is given as

$$\mathcal{Q}_B(\varrho) = \varrho_{i^*} \text{ where } i^* = \arg \min_{i=0, \dots, 2^B-1} |\varrho - \varrho_i|. \quad (45)$$

The parameters ϱ_{\max} and Δ correspond to the maximum quantizer level value and the distance between adjacent quantizer levels, respectively. In our numerical studies, we use $\varrho_{\max} = 30$ dB with $\Delta = 24$ dB for $B = 2$ bits, and $\Delta = 30$ dB for $B = 4$ bits.

A similar approach is pursued in quantizing the amplitudes of the multi-user beam. While these amplitudes do not span a wide range, the relative variation across the antenna array can show wide variations. Specifically, the infinite-precision zeroforcing beams generated in Prop. 1 are quantized to meet the RF constraints in (7) as described next. Since $\|\mathbf{f}_k\| = 1$, we assume that on average $\mathbf{f}_k(i) \approx \frac{1}{\sqrt{N_t}}$. By scaling $|\mathbf{f}_k(i)|^2$ by N_t , we can ensure that $10 \log_{10} (N_t \cdot |\mathbf{f}_k(i)|^2)$ is centered around 0 dB and for this quantity, we generate 2^B quantization levels in dB scale (denoted as f_i) corresponding to a step size of Δf (in dB) as follows:

$$f_i = \Delta f \cdot [i + 1 - 2^{B-1}], \quad i = 0, \dots, 2^B - 1. \quad (46)$$

With these levels that are spaced Δf apart, we obtain the quantized beam weights as

$$|\hat{\mathbf{f}}_k(i)| = \tilde{\mathcal{Q}}_B(|\mathbf{f}_k(i)|) = \frac{1}{\sqrt{N_t}} \cdot \begin{cases} 0 & \text{if } 10 \log_{10} (N_t \cdot |\mathbf{f}_k(i)|^2) < -\Delta f \cdot (2^{B-1} - 1) \\ 10^{\frac{f_{j^*}}{20}} & \text{otherwise,} \end{cases} \quad (47)$$

where

$$j^* = \arg \min_j 10 \log_{10} (N_t \cdot |\mathbf{f}_k(i)|^2) - f_j \text{ provided } 10 \log_{10} (N_t \cdot |\mathbf{f}_k(i)|^2) > f_j. \quad (48)$$

The constraint in (48) ensures that $\sum_i |\hat{\mathbf{f}}_k(i)|^2 \leq 1$. In our numerical studies, we use $\Delta f = 1$ dB for $B = 4$ bits leading to a range of -7 to 8 dB for f_i . We also use $\Delta f = 0.25$ dB for $B = 6$ bits leading to a range of -7.75 to 8 dB for f_i . For the phase quantities (that is, $\tilde{\mathcal{Q}}_B(\angle \mathbf{f}_k(i))$), we reuse $\mathcal{Q}_B(\angle \mathbf{f}_k(i))$ as in (42).

C. Finite-Rate Feedback

With the quantizer design as described in Sec. V-B, we now consider the impact of finite-rate feedback of the quantities of interest necessary for the channel reconstruction step. As noted from Table I, each user quantizes and feeds back to the base-station: i) the base-station beam indices, ii) the received SNRs, iii) the received signal's phases, and iv) user side codebook correlation information (amplitude and phases). To reduce clutter in presentation, in our studies illustrated in Fig. 3, we only focus on the $N = 8$ and $N = 32$ codebooks for beam alignment with $M = 16$ at the user side. Fig. 3(a) considers the impact of B_{SNR} (the number of bits used in received SNR quantization) while infinite-precision is used for the signal phases and codebook correlation. This figure shows that the proposed scheme is robust to B_{SNR} in the sense that for both the $P = 2$ and $P = 4$ cases, the performance improvement is minimal as B_{SNR} is increased from 2 bits to 4 bits.

On the other hand, Fig. 3(b) considers the impact of $B_{\text{est, phase}}$ (the number of bits used in received signal phase quantization) while infinite-precision is used for received SNR and codebook correlation. In the third experiment, we study the impact of codebook correlation quantization with infinite-precision for the other two quantities. To simplify this investigation, we assume that $B_{\text{corr, phase}} = B_{\text{corr, amp}} = B_{\text{corr}}$ and Fig. 3(c) considers the impact of B_{corr} on performance. Both Figs. 3(b) and (c) show that increasing $B_{\text{est, phase}}$ or B_{corr} has maximal impact on performance for large P . In other words, if the channel approximation gets better, it becomes pertinent to quantize the phase terms and codebook correlation information in the channel reconstruction with a finer resolution.

While Figs. 3(a)-(c) study the quantization of each parameter of interest separately, we now consider the impact of finite-rate quantization of all the parameters necessary for channel reconstruction (relative to infinite-precision quantization). For this, we consider the case where $B_{\text{SNR}} = B_{\text{est, phase}} = B_{\text{corr, amp}} = B_{\text{corr, phase}} = 3$ bits with $M = 16$. From Fig. 3(d), we observe that the proposed joint quantization scheme performs comparable with a scheme that uses infinite-precision for all the parameters of interest.

TABLE II: Feedback overhead (B_{feedback}) for different choices of P and N

	$N = 4$	$N = 8$	$N = 16$	$N = 32$
$P = 2$	14	16	18	20
$P = 4$	44	48	52	56

At this stage, it is important to note that the feedback overhead of $\varphi_{k,\ell}$ and $\nu_{k,\ell}$ can be combined⁶ since they are always used in the form $\varphi_{k,\ell} + \nu_{k,\ell}$ (see (24)). Thus, based on the above studies, we make the following heuristic design guidelines on the feedback overhead

$$B_{\text{SNR}} = 2 \text{ bits}, \quad B_{\text{est, phase}} + B_{\text{corr, phase}} = B_{\text{corr, amp}} = P \text{ bits.} \quad (49)$$

Combining this information with Table I, the total feedback overhead from each user is given as

$$B_{\text{feedback}} = P \cdot [\log_2(N) + B_{\text{SNR}} + B_{\text{corr, amp}}] + (P - 1) \cdot [B_{\text{est, phase}} + B_{\text{corr, phase}}] \quad (\text{in bits}) \quad (50)$$

$$= P \cdot [\log_2(N) + 2 + P] + (P - 1) \cdot P \quad (51)$$

$$= P \cdot [\log_2(N) + 2P + 1] \text{ bits.} \quad (52)$$

B_{feedback} is presented in Table II for the choices $P \in \{2, 4\}$ and $N \in \{4, 8, 16, 32\}$. From Table II, a 56 bit control payload appears to be sufficient to convey the information necessary for multi-user beamforming across different choices of M , N and P . On a first glance, while this may appear to be onerous, similar feedback overheads are currently considered viable in 3GPP 5G-NR design. In particular, two types of feedback methods are being studied [41, Sec. 8.2.1.6.3, pp. 24-26]: i) Type-I feedback of both the beam indices and RSRPs of the top-4 beams, and ii) a more general Type-II feedback that can include feedback of covariance matrices, co-phasing factors with different codebook structures, etc. Further, the time-scales at which this information has to be reported is on the order of the coherence time of the channel (which varies from a few milliseconds at high speeds to a few hundreds of milliseconds in an indoor or low speed scenario [10], [40]) allowing multiple long PUCCH instances for beam reporting. Also, this

⁶Similarly, it might be envisioned that the feedback of $\gamma_{k,\ell}$ and $\mu_{k,\ell}$ can be combined, but their dynamic ranges are different. Feedback overhead reduction could be a useful topic of study in future research.

control information can be fed back on legacy carriers such as 4G links in a non-standalone deployment. Thus, the feedback overhead necessary for realizing the proposed schemes are practically viable.

D. Quantization of Multi-User Beams and Comparison with Upper Bounds

In the third study, the effect of quantizing the multi-user beams to ensure that it fits the RF precoder constraints as in (7) is considered. In general, if a low rate quantization is used (B_{amp} or B_{phase}) as P increases, the resultant multi-user beam's sum rate performance could be worse than that with beam steering. In particular, from Fig. 4(a), we observe that a higher phase resolution (B_{phase}) is necessary for improved performance as the codebook resolution improves (large N) or when P increases. On the other hand, from Fig. 4(b), we observe that an amplitude resolution (B_{amp}) on the order of 4-6 bits can produce a performance comparable with the unquantized scheme.

In Fig. 5, we finally compare the performance of the proposed zeroforcing scheme with the beam steering scheme and the bounds established in Sec. IV. We also benchmark the performance with a fully-digital system employing: i) maximal ratio transmission/maximal ratio combining (MRT/MRC) beams in the initial alignment phase, and ii) a zeroforcing scheme performed using the MRT/MRC beams as in [23], [24]. Note that the MRT/MRC scheme is different from that employed in [23], [24] where perfect beam steering vectors are used in deriving the zeroforcing structure. In terms of differences between these structures, the readers are referred to [18]. For the proposed scheme, an $M = 16$ codebook is used at the user end. Figs. 5(a)-(b) and Fig. 6 illustrate the trends with $N = 8$, $N = 32$, and $N = 256$ codebooks, respectively. For $N = 256$, we employ a DFT codebook at the base-station covering the $120^\circ \times 30^\circ$ AoD space.

With low-resolution quantization, we note that there is a considerable performance gap between the zeroforcing scheme and the scalar optimization-based upper bound (up to 2 bps/Hz). On the other hand, this gap reduces as N increases suggesting the good performance of the zeroforcing scheme. Nevertheless, the performance gap between the proposed zeroforcing scheme and the upper bounds suggests the possible utility of more advanced feedback mechanisms, a topic for future research. In all the plots, there is a considerable gap between the performance of the upper bounds with the fully-digital system. Plausible explanations for this observation include the use of small arrays at the user end (2×2) and $L_k = 6$ clusters in the channel. A more complex hybrid precoding architecture achieved by optimally choosing \mathbf{F}_{Dig} with respect to

some performance metric may assist in bridging this gap. It is also to be pointed out that while the alternate optimization-based sum rate serves as an upper bound for most channel realizations, for some realizations (especially at low SINR values where the SLNR optimization has a different behavior than the sum rate maximization), this connection breaks down.

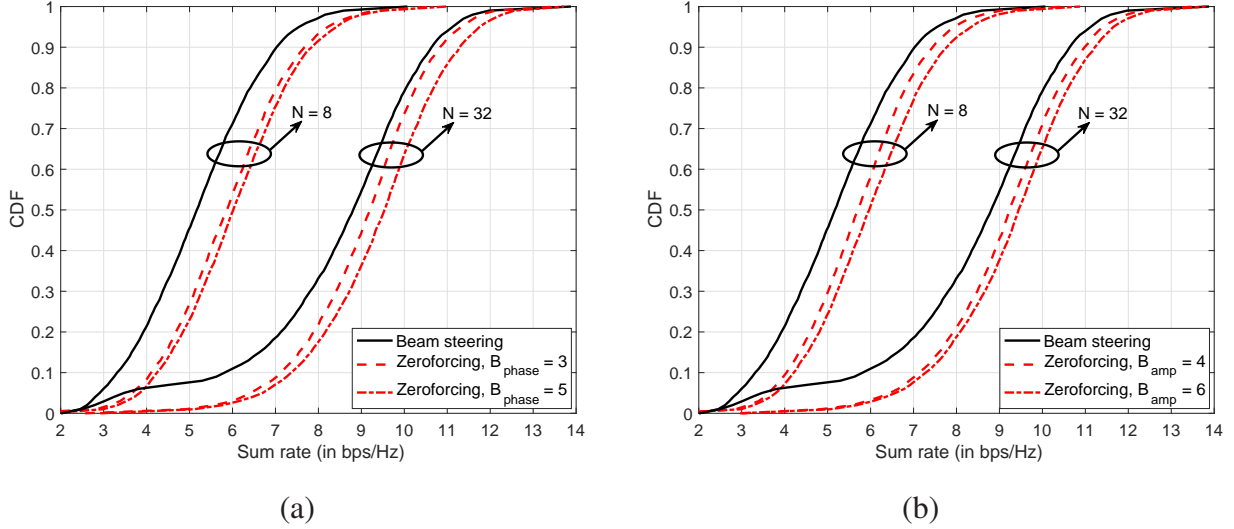


Fig. 4: CDF of sum rates of the different schemes with quantization constraints on the multi-user beam's (a) phases and (b) amplitudes.

VI. CONCLUDING REMARKS

The focus of this work has been the development of a feedback mechanism to convey estimates of certain quantities of interest from an initial beam alignment phase to enable the base-station to construct an advanced RF precoding structure for multi-user transmissions. These quantities of interest include the top- P (where $P \geq 1$) base-station side beam indices, phases and amplitudes of an appropriate received signal estimate, as well as the cross-correlation information of the beams at the user end. This feedback is leveraged to reconstruct/estimate a rank- P approximation of the channel matrix of interest at the base-station end and generate a zeroforcing structure for multi-user interference management. Numerical studies show that the additional feedback overhead is marginal, but the relative performance improvement over a simplistic beam steering scheme is significant even with a very coarse initial beam alignment codebook.

This study reinforces the importance of the development of low-complexity (in terms of feedback overhead as well as implementation) yet good (in terms of performance and structure)

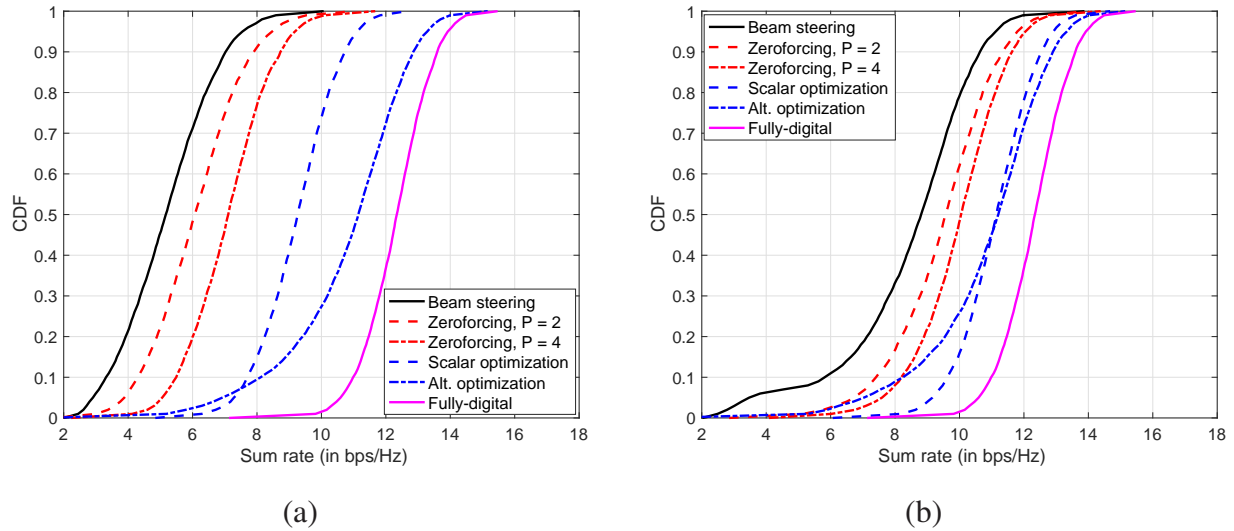


Fig. 5: CDF of sum rates of the multi-user schemes compared with the two upper bounds using a $M = 16$ codebook with (a) $N = 8$, (b) $N = 32$.

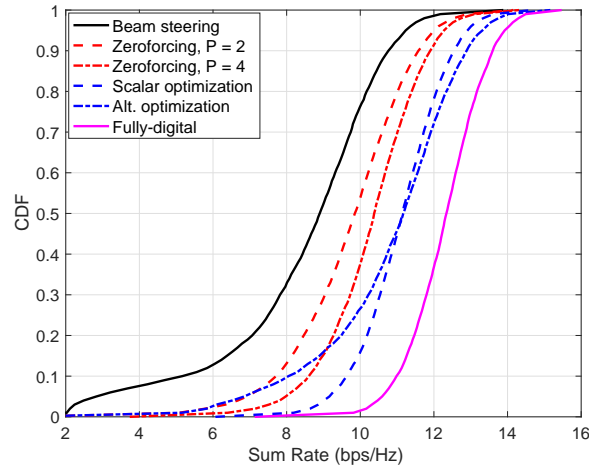


Fig. 6: CDF of sum rates of the multi-user schemes compared with the two upper bounds using a $M = 16$ codebook with $N = 256$.

feedback techniques for large-MIMO systems [47], [48]. While this work has only scratched the surface of such techniques, a number of possible future research directions are worth considering. Benchmarking the performance of any proposed feedback technique with a tight upper bound (for the sum rate) is an area of fundamental difficulties due to the non-convex nature of the problem [42]–[44] and is richly rewarding. Understanding the fundamental limits of hybrid

precoders beyond the phase-only control architecture that is common in the literature, as well as providing a directional intuition into the structure of the precoder construction (in contrast to a *black box* optimization solution) are of importance in practical implementations. While the solutions proposed in this work can be readily extended to polarization-diversity transmissions, extending it to the case where the users possess two (or more) RF chains with the base-station communicating over two *spatial* layers is of importance from a 3GPP 5G-NR deployment perspective. Study of different hybrid beamforming architectures such as the sub-connected structure in [35] and comparison with the proposed scheme(s) would be of interest. Sensitivity of such advanced schemes to impairments such as Doppler and phase noise are also worth exploring more carefully.

APPENDIX

A. Generalized Eigenvector Solution

We need the following statement on the generalized eigenvector solution to the standard optimization that will be repeatedly considered in this work.

Lemma 1. *If \mathbf{B} is an $n \times n$ positive definite matrix, then the principal square-root (denoted as $\mathbf{B}^{1/2}$) exists and is invertible (denoted as $\mathbf{B}^{-1/2}$). Further, if \mathbf{A} is another $n \times n$ positive semi-definite matrix, the following optimization over $n \times 1$ unit-norm vectors is well-understood [24], [44]*

$$\mathbf{f}_{\text{opt}} = \arg \max_{\mathbf{f}: \|\mathbf{f}\|=1} \frac{\mathbf{f}^\dagger \mathbf{A} \mathbf{f}}{\mathbf{f}^\dagger \mathbf{B} \mathbf{f}} = \frac{\mathbf{B}^{-1/2} \cdot \text{Dom eig}(\mathbf{B}^{-1/2} \mathbf{A} \mathbf{B}^{-1/2})}{\|\mathbf{B}^{-1/2} \cdot \text{Dom eig}(\mathbf{B}^{-1/2} \mathbf{A} \mathbf{B}^{-1/2})\|} \quad (53)$$

with $\text{Dom eig}(\cdot)$ denoting the dominant eigenvector operation of the underlying matrix. In the special case where $\mathbf{A} = \mathbf{w} \mathbf{w}^\dagger$ is a rank-1 matrix for some column vector \mathbf{w} , then \mathbf{f}_{opt} reduces to $\mathbf{f}_{\text{opt}} = \frac{\mathbf{B}^{-1} \mathbf{w}}{\|\mathbf{B}^{-1} \mathbf{w}\|}$. \square

Note that the generalized eigenvector of a matrix pair (\mathbf{A}, \mathbf{B}) is a vector \mathbf{x} that solves the problem $\mathbf{A} \mathbf{x} = \sigma \mathbf{B} \mathbf{x}$ for some scalar σ . From this description, it can be seen that \mathbf{f}_{opt} in (53) is the dominant unit-norm generalized eigenvector of the matrix pair (\mathbf{A}, \mathbf{B}) .

B. Proof of Prop. 1

Given the expression for $\widehat{\text{SINR}}_m$ in (20), the zeroforcing structure corresponds to the construction $\{\mathbf{f}_m\}$ such that

$$|\mathbf{g}_k^\dagger \widehat{\mathbf{H}}_k \mathbf{f}_m|^2 = 0, \quad m \neq k, \quad \{m, k\} \in 1, \dots, K. \quad (54)$$

An elementary computation shows that by setting $\mathbf{f}_m, m = 1, \dots, K$ as in the statement of the proposition, we can ensure the condition in (54). \square

C. Proof of Prop. 2

Since $\mathbf{f}_k^\dagger \mathbf{f}_k = 1$, we can write $\widehat{\text{SLNR}}_k$ as

$$\widehat{\text{SLNR}}_k = \frac{\eta_{k,k} \cdot \mathbf{f}_k^\dagger \cdot \left(\widehat{\mathbf{H}}_k^\dagger \mathbf{g}_k \mathbf{g}_k^\dagger \widehat{\mathbf{H}}_k \right) \cdot \mathbf{f}_k}{\mathbf{f}_k^\dagger \cdot \left(\mathbf{I}_{N_t} + \sum_{m \neq k} \eta_{m,k} \widehat{\mathbf{H}}_m^\dagger \mathbf{g}_m \mathbf{g}_m^\dagger \widehat{\mathbf{H}}_m \right) \cdot \mathbf{f}_k}. \quad (55)$$

The optimal structure of \mathbf{f}_k in the statement of the proposition follows directly from Lemma 1. \square

REFERENCES

- [1] F. Khan and Z. Pi, “An introduction to millimeter wave mobile broadband systems,” *IEEE Commun. Magaz.*, vol. 49, no. 6, pp. 101–107, June 2011.
- [2] N. Bhushan, J. Li, D. Malladi, R. Gilmore, D. Brenner, A. Damnjanovic, R. T. Sukhasvi, C. Patel, and S. Geirhofer, “Network densification: The dominant theme for wireless evolution into 5G,” *IEEE Commun. Magaz.*, vol. 52, no. 2, pp. 82–89, Feb. 2014.
- [3] T. S. Rappaport, S. Sun, R. Mayzus, H. Zhao, Y. Azar, K. Wang, G. N. Wong, J. K. Schulz, M. K. Samimi, and F. Gutierrez, “Millimeter wave mobile communications for 5G cellular: It will work!,” *IEEE Access*, vol. 1, pp. 335–349, 2013.
- [4] F. Boccardi, R. W. Heath, Jr., A. Lozano, T. L. Marzetta, and P. Popovski, “Five disruptive technology directions for 5G,” *IEEE Commun. Magaz.*, vol. 52, no. 2, pp. 74–80, Feb. 2014.
- [5] Aalto University, AT&T, BUPT, CMCC, Ericsson, Huawei, Intel, KT Corporation, Nokia, NTT DOCOMO, NYU, Qualcomm, Samsung, U. Bristol, and USC, “White paper on ‘5G channel model for bands up to 100 GHz,’” v2.3, Oct. 2016.
- [6] 3GPP TR 38.901 V14.1.1 (2017-07), “Technical Specification Group Radio Access Network; Study on Channel Model for Frequencies from 0.5 to 100 GHz (Rel. 14),” July 2017.
- [7] Y. Azar, G. N. Wong, K. Wang, R. Mayzus, J. K. Schulz, H. Zhao, F. J. Gutierrez, D. Hwang, and T. S. Rappaport, “28 GHz propagation measurements for outdoor cellular communications using steerable beam antennas in New York City,” *Proc. IEEE Intern. Conf. Commun., Budapest, Hungary*, pp. 5143–5147, June 2013.
- [8] S. Sun, T. S. Rappaport, T. A. Thomas, A. Ghosh, H. C. Nguyen, I. Z. Kovács, I. Rodriguez, O. H. Koymen, and A. Partyka, “Investigation of prediction accuracy, sensitivity, and parameter stability of large-scale propagation path loss models for 5G wireless communications,” *IEEE Trans. Veh. Tech.*, vol. 65, no. 5, pp. 2843–2860, May 2016.
- [9] V. Raghavan, A. Partyka, L. Akhoondzadeh-Asl, M. A. Tassoudji, O. H. Koymen, and J. Sanelli, “Millimeter wave channel measurements and implications for PHY layer design,” *IEEE Trans. Ant. Propagat.*, vol. 65, no. 12, pp. 6521–6533, Dec. 2017.
- [10] V. Raghavan, L. Akhoondzadeh-Asl, V. Podshivalov, J. Hulten, M. A. Tassoudji, O. H. Koymen, A. Sampath, and J. Li, “Statistical blockage modeling and robustness of beamforming in millimeter wave systems,” *Submitted to IEEE Trans. Ant. Propagat.*, Available: [Online]. <https://arxiv.org/abs/1801.03346>.

- [11] V. Raghavan and A. M. Sayeed, "Sublinear capacity scaling laws for sparse MIMO channels," *IEEE Trans. Inf. Theory*, vol. 57, no. 1, pp. 345–364, Jan. 2011.
- [12] Qualcomm, "Clustering methodology and results based on omni-directional and azimuthal scans in 29 and 61 GHz," *R1-161666, 3GPP TSG RAN WG1 #AH Channel Model, Ljubljana, Slovenia*, Mar. 2016.
- [13] F. Rusek, D. Persson, B. K. Lau, E. G. Larsson, T. L. Marzetta, O. Edfors, and F. Tufvesson, "Scaling up MIMO: Opportunities and challenges with very large arrays," *IEEE Sig. Proc. Magaz.*, vol. 30, no. 1, pp. 40–60, Jan. 2013.
- [14] S. Hur, T. Kim, D. J. Love, J. V. Krogmeier, T. A. Thomas, and A. Ghosh, "Millimeter wave beamforming for wireless backhaul and access in small cell networks," *IEEE Trans. Commun.*, vol. 61, no. 10, pp. 4391–4403, Oct. 2014.
- [15] W. Roh, J.-Y. Seol, J. Park, B. Lee, J. Lee, Y. Kim, J. Cho, K. Cheun, and F. Aryanfar, "Millimeter-wave beamforming as an enabling technology for 5G cellular communications: Theoretical feasibility and prototype results," *IEEE Commun. Magaz.*, vol. 52, no. 2, pp. 106–113, Feb. 2014.
- [16] J. Brady, N. Behdad, and A. M. Sayeed, "Beamspace MIMO for millimeter-wave communications: System architecture, modeling, analysis and measurements," *IEEE Trans. Ant. Propagat.*, vol. 61, no. 7, pp. 3814–3827, July 2013.
- [17] O. El Ayach, S. Rajagopal, S. Abu-Surra, Z. Pi, and R. W. Heath, Jr., "Spatially sparse precoding in millimeter wave MIMO systems," *IEEE Trans. Wireless Commun.*, vol. 13, no. 3, pp. 1499–1513, Mar. 2014.
- [18] V. Raghavan, S. Subramanian, J. Cezanne, and A. Sampath, "Directional beamforming for millimeter-wave MIMO systems," *Proc. IEEE Global Telecommun. Conf., San Diego, CA*, pp. 1–7, Dec. 2015, Extended version: [Online]. <http://www.arxiv.org/abs/1601.02380>.
- [19] V. Raghavan, J. Cezanne, S. Subramanian, A. Sampath, and O. H. Koymen, "Beamforming tradeoffs for initial UE discovery in millimeter-wave MIMO systems," *IEEE Journ. Sel. Topics in Sig. Proc.*, vol. 10, no. 3, pp. 543–559, Apr. 2016.
- [20] S. Rangan, T. S. Rappaport, and E. Erkip, "Millimeter wave cellular networks: Potentials and challenges," *Proc. IEEE*, vol. 102, no. 3, pp. 366–385, Mar. 2014.
- [21] A. Ghosh, T. A. Thomas, M. C. Cudak, R. Ratasuk, P. Moorut, F. W. Vook, T. S. Rappaport, G. R. MacCartney, Jr., S. Sun, and S. Nie, "Millimeter-wave enhanced local area systems: A high data-rate approach for future wireless networks," *IEEE Journ. Sel. Areas in Commun.*, vol. 32, no. 6, pp. 1152–1163, June 2014.
- [22] S. Sun, T. S. Rappaport, R. W. Heath, Jr., A. Nix, and S. Rangan, "MIMO for millimeter wave wireless communications: Beamforming, spatial multiplexing, or both?," *IEEE Commun. Magaz.*, vol. 52, no. 12, pp. 110–121, Dec. 2014.
- [23] V. Raghavan, S. Subramanian, J. Cezanne, A. Sampath, O. H. Koymen, and J. Li, "Directional hybrid precoding in millimeter-wave MIMO systems," *Proc. IEEE Global Telecommun. Conf., Washington, DC*, pp. 1–7, Dec. 2016.
- [24] V. Raghavan, S. Subramanian, J. Cezanne, A. Sampath, O. H. Koymen, and J. Li, "Single-user vs. multi-user precoding for millimeter wave MIMO systems," *IEEE Journ. Sel. Areas in Commun.*, vol. 35, no. 6, pp. 1387–1401, June 2017.
- [25] A. Li and C. Masouros, "Hybrid precoding and combining design for millimeter-wave multi-user MIMO based on SVD," *Proc. IEEE Intern. Conf. on Commun., Paris, France*, pp. 1–6, May 2017.
- [26] X. Zhang, A. F. Molisch, and S. Y. Kung, "Variable-phase-shift-based RF-baseband codesign for MIMO antenna selection," *IEEE Trans. Sig. Proc.*, vol. 53, no. 11, pp. 4091–4103, Nov. 2005.
- [27] P. Sudarshan, N. B. Mehta, A. F. Molisch, and J. Zhang, "Channel statistics-based joint RF-baseband design for antenna selection for spatial multiplexing," *IEEE Trans. Wireless Commun.*, vol. 5, no. 12, pp. 3501–3511, Dec. 2006.
- [28] V. Venkateswaran and A.-J. van der Veen, "Analog beamforming in MIMO communications with phase shift networks and online channel estimation," *IEEE Trans. Sig. Proc.*, vol. 58, no. 8, pp. 4131–4143, Aug. 2010.
- [29] A. Adhikary, E. Al Safadi, M. K. Samimi, R. Wang, G. Caire, T. S. Rappaport, and A. F. Molisch, "Joint spatial division and multiplexing for mm-Wave channels," *IEEE Journ. Sel. Areas in Commun.*, vol. 32, no. 6, pp. 1239–1255, June 2014.

- [30] A. Alkhateeb, O. El Ayach, G. Leus, and R. W. Heath, Jr., "Channel estimation and hybrid precoding for millimeter wave cellular systems," *IEEE Journ. Sel. Topics in Sig. Proc.*, vol. 8, no. 5, pp. 831–846, Oct. 2014.
- [31] A. Alkhateeb, G. Leus, and R. W. Heath, Jr., "Limited feedback hybrid precoding for multi-user millimeter wave systems," *IEEE Trans. Wireless Commun.*, vol. 14, no. 11, pp. 6481–6494, Nov. 2015.
- [32] F. Sohrabi and W. Yu, "Hybrid digital and analog beamforming design for large-scale antenna arrays," *IEEE Journ. Sel. Topics in Sig. Proc.*, vol. 10, no. 3, pp. 501–513, Apr. 2016.
- [33] S. Noh, M. D. Zoltowski, and D. J. Love, "Training sequence design for feedback assisted hybrid beamforming in massive MIMO systems," *IEEE Trans. Commun.*, vol. 64, no. 1, pp. 187–200, Jan. 2016.
- [34] T. E. Bogale, L. B. Le, A. Haghighat, and L. Vandendorpe, "On the number of RF chains and phase shifters, and scheduling design with hybrid analog-digital beamforming," *IEEE Trans. Wireless Commun.*, vol. 15, no. 5, pp. 3311–3326, May 2016.
- [35] X. Gao, L. Dai, S. Han, C-L. I, and R. W. Heath, Jr., "Energy-efficient hybrid analog and digital precoding for mmWave MIMO systems with large antenna arrays," *IEEE Journ. Sel. Areas in Commun.*, vol. 34, no. 4, pp. 998–1009, Apr. 2016.
- [36] R. L. Magueta, D. Castanheira, A. Silva, R. Dinis, and A. Gameiro, "Hybrid iterative space-time equalization for multi-user mmW massive MIMO systems," *IEEE Trans. Commun.*, vol. 65, no. 2, pp. 608–620, Feb. 2017.
- [37] H. Krishnaswamy and H. Hashemi, "Integrated beamforming arrays," *In mm-Wave Silicon Technology*, (A. M. Niknejad and H. Hashemi, Eds.), Springer, NY, pp. 243–295, 2008.
- [38] G-L. Huang, S-G. Zhou, T-H. Chio, H-T. Hui, and T-S. Yeo, "A low profile and low sidelobe wideband slot antenna array fed by an amplitude-tapering waveguide feed-network," *IEEE Trans. Ant. Propagat.*, vol. 63, no. 1, pp. 419–423, Jan. 2015.
- [39] Z. Briqech, A-R. Sebak, and T. A. Denidni, "Low-cost wideband mmWave phased array using the piezoelectric transducer for 5G applications," *IEEE Trans. Ant. Propagat.*, vol. 65, no. 12, pp. 6403–6412, Dec. 2017.
- [40] V. Raghavan, A. Partyka, S. Subramanian, A. Sampath, O. H. Koymen, K. Ravid, J. Cezanne, K. K. Mukkavilli, and J. Li, "Millimeter wave MIMO prototype: Measurements and experimental results," *IEEE Commun. Magaz.*, vol. 56, no. 1, pp. 202–209, Jan. 2018.
- [41] 3GPP TR 38.912 V14.1.0 (2017-06), "Technical Specification Group Radio Access Network; Study on New Radio (NR) access technology (Rel. 14)," June 2017.
- [42] S. S. Christensen, R. Agarwal, E. de Carvalho, and J. M. Cioffi, "Weighted sum-rate maximization using weighted MMSE for MIMO-BC beamforming design," *IEEE Trans. Wireless Commun.*, vol. 7, no. 12-1, pp. 4792–4799, Dec. 2008.
- [43] M. Kobayashi and G. Caire, "An iterative water-filling algorithm for maximum weighted sum-rate of Gaussian MIMO-BC," *IEEE Journ. Sel. Areas in Commun.*, vol. 24, no. 8, pp. 1640–1646, Aug. 2006.
- [44] V. Raghavan, S. V. Hanly, and V. V. Veeravalli, "Statistical beamforming on the Grassmann manifold for the two-user broadcast channel," *IEEE Trans. Inf. Theory*, vol. 59, no. 10, pp. 6464–6489, Oct. 2013.
- [45] M. Sadek, A. Tarighat, and A. H. Sayed, "A leakage-based precoding scheme for downlink multi-user MIMO channels," *IEEE Trans. Wireless Commun.*, vol. 6, no. 5, pp. 1711–1721, May 2007.
- [46] A. A. M. Saleh and R. Valenzuela, "A statistical model for indoor multipath propagation," *IEEE Journ. Selected Areas in Commun.*, vol. 5, no. 2, pp. 128–137, Feb. 1987.
- [47] D. J. Love, R. W. Heath, Jr., V. K. N. Lau, D. Gesbert, B. D. Rao, and M. Andrews, "An overview of limited feedback in wireless communication systems," *IEEE Journ. Selected Areas in Commun.*, vol. 26, no. 8, pp. 1341–1365, Oct. 2008.
- [48] V. Raghavan, J. J. Choi, and D. J. Love, "Design guidelines for limited feedback in the spatially correlated broadcast channel," *IEEE Trans. Commun.*, vol. 63, no. 7, pp. 2524–2540, July 2015.

- [49] J. Song, J. J. Choi, and D. J. Love, "Common codebook millimeter wave beam design: Designing beams for both sounding and communication with uniform planar arrays," *IEEE Trans. Commun.*, vol. 65, no. 4, pp. 1859–1872, Apr. 2017.
- [50] S. Noh, M. D. Zoltowski, and D. J. Love, "Multi-resolution codebook and adaptive beamforming sequence design for millimeter wave beam alignment," *IEEE Trans. Wireless Commun.*, vol. 16, no. 9, pp. 5689–5701, Sept. 2017.
- [51] A. M. Sayeed, "Deconstructing multi-antenna fading channels," *IEEE Trans. Sig. Proc.*, vol. 50, no. 10, pp. 2563–2579, Oct. 2002.
- [52] A. M. Tulino, A. Lozano, and S. Verdú, "Impact of antenna correlation on the capacity of multiantenna channels," *IEEE Trans. Inf. Theory*, vol. 51, no. 7, pp. 2491–2509, July 2005.